Science of the Total Environment 586 (2017) 372–389

Contents lists available at ScienceDirect

Science of the Total Environment

journal homepage: www.elsevier.com/locate/scitotenv

Groundwater nitrate reduction versus dissolved gas production: A tale of two catchments

E.B. McAleer [a,b,c,*], C.E. Coxon [a], K.G. Richards [c,*], M.M.R Jahangir [c], J. Grant [d], Per.E. Mellander [b]

[a] Geology Department/Trinity Centre for the Environment, School of Natural Sciences, Trinity College Dublin, Dublin 2, Ireland
[b] Agricultural Catchments Programme, Teagasc, Environment Research Centre, Johnstown Castle, Wexford, Ireland
[c] Crops, Environment and Land Use Programme, Teagasc Environment Research Centre, Johnstown Castle, Wexford, Ireland
[d] Teagasc, Ashtown Food Research Centre, Dublin, Ireland

HIGHLIGHTS

- NO_3^- removal capacity was highly variable between and within study catchments.
- Hydrogeological and agronomic factors controlled groundwater hydrogeochemical signatures.
- NO_3^- consumption was coupled with excess N_2 and N_2O production.
- Excess N_2 was the dominant denitrification reaction product in near stream groundwater.
- Groundwater N_2O was a net source of greenhouse gas emissions in both catchments.

GRAPHICAL ABSTRACT

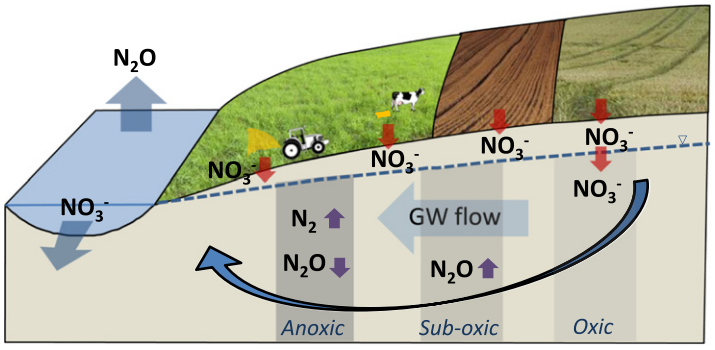

ARTICLE INFO

Article history:
Received 6 September 2016
Received in revised form 13 November 2016
Accepted 14 November 2016
Available online 20 February 2017

Editor: D. Barcelo

Keywords:
Denitrification
Excess N_2
N_2O
Dissolved oxygen
Pollutant swapping
Agriculture

ABSTRACT

At the catchment scale, a complex mosaic of environmental, hydrogeological and physicochemical characteristics combine to regulate the distribution of groundwater and stream nitrate (NO_3^-). The efficiency of NO_3^- removal (via denitrification) versus the ratio of accumulated reaction products, dinitrogen (excess N_2) & nitrous oxide (N_2O), remains poorly understood. Groundwater was investigated in two well drained agricultural catchments (10 km^2) in Ireland with contrasting subsurface lithologies (sandstone vs. slate) and landuse. Denitrification capacity was assessed by measuring concentration and distribution patterns of nitrogen (N) species, aquifer hydrogeochemistry, stable isotope signatures and aquifer hydraulic properties. A hierarchy of scale whereby physical factors including agronomy, water table elevation and permeability determined the hydrogeochemical signature of the aquifers was observed. This hydrogeochemical signature acted as the dominant control on denitrification reaction progress. High permeability, aerobic conditions and a lack of bacterial energy sources in the slate catchment resulted in low denitrification reaction progress (0–32%), high NO_3^- and comparatively low N_2O emission factors ($EF_{5g}1$). In the sandstone catchment denitrification progress ranged from 4 to 94% and was highly dependent on permeability, water table elevation, dissolved oxygen concentration solid phase bacterial energy sources. Denitrification of NO_3 — to N_2 occurred in anaerobic conditions, while at intermediate dissolved oxygen; N_2O was the dominant reaction product. $EF_{5g}1$ (mean: 0.0018) in the denitrifying sandstone catchment was 32% less than the IPCC default. The denitrification observations across catchments were supported by stable isotope signatures. Stream NO_3^- occurrence was 32% lower in the sandstone catchment even though N loading was substantially higher than the slate catchment.

* Corresponding authors at: Teagasc Environment Research Centre, Johnstown Castle, Wexford Town, Ireland.
E-mail addresses: e.mcaleer1@gmail.com (E.B. McAleer), Karl.Richards@teagasc.ie (K.G. Richards).

http://dx.doi.org/10.1016/j.scitotenv.2016.11.083

1. Introduction

Anthropogenic application of inorganic and organic nitrogen (N) fertilisers to agricultural landscapes has pervasive consequences including human health implications (e.g. methemoglobinaemia), eutrophication, aquatic acidification, loss of habitat biodiversity and greenhouse gas emissions (Dennis et al., 2012; Gruber and Galloway, 2008; Richards et al., 2015; Weymann et al., 2008). In light of agricultural intensification, the identification of subsurface environments with a natural capacity to attenuate excess N is essential to the development of sustainable management strategies. Globally, denitrification is regarded as the dominant nitrate (NO_3^-) attenuation mechanism in groundwater (Korom, 1992; Rivett et al., 2008; Seitzinger et al., 2006). Denitrification is a microbially mediated process whereby NO_3^- is reduced to dinitrogen (N_2) gas. In baseflow dominated catchments, groundwater denitrification has the capacity to mitigate stream water N enrichment by returning N to the long residence time atmospheric pool (Heffernan et al., 2012). Denitrification can represent an environmentally positive nitrate removal process (Schipper and Vojvodić-Vuković, 2001); however such a characterisation is subject to an important caveat. The reaction is sequential and as such there are several intermediary products including nitrite (NO_2^-), nitric oxide (NO) and nitrous oxide (N_2O). The differentiation between which reaction product is dominant is of key environmental concern: N_2 gas is environmentally benign whereas N_2O is a potent greenhouse gas, while NO contributes to stratospheric ozone depletion, eutrophication and formation and accumulation of surface ozone (Vitousek et al., 1997).

In groundwater, a number of geochemical criteria must be met for denitrification to occur. Studies documenting the relationship between NO_3^- concentrations and aquifer physicochemistry are prevalent in the available literature (Brettar et al., 2002; Jahangir et al., 2012a; Rissmann, 2011). A commonality throughout indicates that the presence of denitrifying bacteria, reducing conditions and the availability of bacterial energy sources create zones of enhanced denitrification potential. Traditionally, it has been believed that that groundwater denitrification is predominantly heterotrophic with rates related to the amount of dissolved organic carbon (DOC) coupled with the wide abundance of denitrifiers in the groundwater (Barrett et al., 2013; Rivett et al., 2008). Recent research however suggests that autotrophic denitrification i.e. oxidation of solid phases within an aquifer such as Iron (Fe) and Manganese (Mn) may in fact drive bacterial NO_3^- reduction (Green et al., 2008; Heffernan et al., 2012). Great uncertainty surrounds the spatial and temporal distribution of denitrifying zones, owing to a confounding hierarchy of scale. In essence, an aquifer can be visualised as an environmental ecosystem, which is capable of removing between 0 and 100% of reactive N. The geological history of the aquifer (mineralogy, stratigraphy and weathering) at the catchment scale controls the distribution and availability of bacterial energy sources, aquifer flow paths, permeability and connectivity at the sub metre scale (Seitzinger et al., 2006). These physical factors in turn determine the hydrogeochemical signature and N attenuating capacity of the aquifer, while agronomy, soil type, hillslope geometry and meteorology control the temporal N load passing through the ecosystem. In complex geological environments, an entire aquifer or catchment cannot be characterised as having high or low denitrification potential. Denitrification is enhanced in certain spatial zones or hot spots (Jahangir et al., 2012a, 2013) and it is the location and intensity of these hot spots in relation to a receptor e.g. a stream, which is paramount to characterising the potential for natural attenuation of N in an aquifer. Several studies have measured denitrification based upon NO_3^- loss (Jahangir et al., 2012a; Thayalakumaran et al., 2008; Tsushima et al., 2002), however NO_3^- gradients can result from temporal patterns of source contribution (Seitzinger et al., 2006) and other NO_3^- removal pathways such as plant and microbial assimilation, dissimilatory NO_3^- reduction to ammonium (NH_4^+) and anaerobic oxidation of NH_4^+ (Jahangir et al., 2016). Studies based solely on NO_3^- dynamics have a capacity to overestimate the contribution of denitrification on NO_3^- removal rates (Green et al., 2008). Directly measured denitrification rates based upon the natural accumulation of denitrification products (N_2O & N_2) in groundwater are rare with calculated values spanning orders of magnitude across studies (Green et al., 2008; Heffernan et al., 2012; Jahangir et al., 2013; Weymann et al., 2008). $^{15}N_{NO3}$ isotopic signatures have been used extensively to calculate N sources and processes (Kendall et al., 2007). A dual isotopic approach ($^{15}N_{NO3}$ and $^{18}O_{NO3}$) can be used to infer both the source of NO_3^- to groundwater and also transformational processes such as denitrification (Wassenaar, 1995). Although it is not possible to directly calculate denitrification rates from isotopic signatures, coupled enrichment of $^{15}N_{NO3}$ and $^{18}O_{NO3}$ provides a powerful tool to identify areas of enhanced denitrification (Baily et al., 2011).

Contemporaneous measurements of both N_2O and N_2 in groundwater not only provide evidence of NO_3^- removal pathways but also offer an insight into the concept of pollutant swapping of NO_3^- for N_2O. Globally it is estimated that agricultural practises are responsible for in excess of 60% of anthropogenic N_2O emissions (Harty et al., 2016). The International Panel on Climate Change (IPCC) subdivides agricultural N_2O into three categories: direct emissions from agricultural land, emissions from animal management strategies and indirect emissions of N_2O that is either volatilised, leached or removed in biomass (IPCC, 1997). Each subcategory is estimated to contribute one third of the total agricultural N_2O source with indirect emission estimations contributing two thirds of the uncertainty (Penman, 2000). There exists a substantial body of research into the contribution N_2O to the global greenhouse gas budget via direct pathways i.e. from soil to the atmosphere (Bouwman, 1990; de Klein et al., 2001; Li et al., 2011, 2013; Soussana et al., 2007). Large uncertainties remain around the contribution of indirect N_2O emission pathways, namely from groundwater and surface drainage, rivers and coastal marine areas (Vilain et al., 2012). Fuelling this uncertainty is a lack of process based understanding regarding the production, consumption and movement of groundwater and stream N_2O across a range of hydrogeological settings (Clough et al., 2007; Höll et al., 2005; Jahangir et al., 2013). In 1997, the IPCC published an emission factor of 0.015 for the fraction of agriculturally derived N_2O released from groundwater sources (Mosier et al., 1999). In 2006, the IPCC default value was amended to 0.0025 (de Klein et al., 2006) based upon the combined reviews of Hiscock et al. (2003), Reay et al. (2005) and Sawamoto et al. (2005). While this downward revision indicated that groundwater derived N_2O was less significant than previously proposed, the published range of uncertainty (0.0005–0.025) highlighted the ambiguity surrounding the natural variability of N_2O in groundwater while reinforcing the need for further research to constrain emission factors and reduce uncertainty. Studies combining a complete analysis of N species: organic N, ammonium (NH_4^+–N), NO_3^-–N, nitrite (NO_2^-–N), N_2O–N & N_2–N, with aerobicity (dissolved oxygen and redox potential), electron donors, dual isotopic techniques and aquifer hydraulic properties are rare. It is only through the refinement of scale, from catchment to sub metre, that a process based understanding of groundwater N removal can be developed.

The objectives of this study are (1) to quantify the capacity of hillslope hydrologic systems to naturally attenuate agriculturally derived NO_3^-, 2) to elucidate the extent of denitrification by measuring the accumulation and ratio of reaction products (N_2 and N_2O) and (3) to identify the physical and biogeochemical factors affecting groundwater denitrification rates and indirect N_2O emissions from groundwater.

2. Materials & methods

2.1. Study sites

This research was undertaken along four hillslopes of varying length, geometry and landuse in two agricultural catchments in the Republic of

Ireland (Fig. 1). The catchments, termed herein as sandstone and slate, were chosen to represent the dominant Irish land use categories in landscapes susceptible to potential phosphorous and nitrogen transfer risk (Fealy et al., 2010). The sandstone catchment is characterised by intensive dairy grassland agriculture, while continuous arable crop production dominates the slate catchment. Within both study catchments, two instrumented hillslopes termed *Sandstone N*/*Sandstone S* and *Slate N*/*Slate S* were targeted to represent general catchment morphology and land use with each exhibiting a range of hydrogeochemical conditions. Each hillslope intersects with a stream channel at its base, representing the receptor or end point for up gradient hydrogeochemical dynamics. A conceptual geological understanding was developed using a suite of geophysical techniques including ground penetrating radar, electromagnetic terrain conductivity, 2D resistivity and seismic refraction (Mellander et al., 2014).

2.2. Monitoring wells

Multilevel monitoring wells were installed in the near stream, midslope and upslope zones of each hillslope (Mellander et al., 2014). In total 12 multilevel wells were installed, each generally comprising three piezometers, yielding a total of 36 sampling intervals. The piezometers (inner diameter: 52 mm) had screened sections ranging in length between one and four metres (typically three metres). The depth to the bottom of each well screened interval ranged in depth from 3.5 to 40 m below ground level (m BGL). The wells screens were targeted to intercept shallow (1–10 m BGL) and deeper bedrock groundwater pathways (10–40 m BGL). Saturated hydraulic conductivity (Ksat) was measured within each screened interval using the slug testing procedure outlined in Butler (1997). Ksat was calculated from the generated time-drawdown data using the Bower and Rice (1976)\ method for unconfined aquifers. Fig. 1 illustrates the experimental design and location

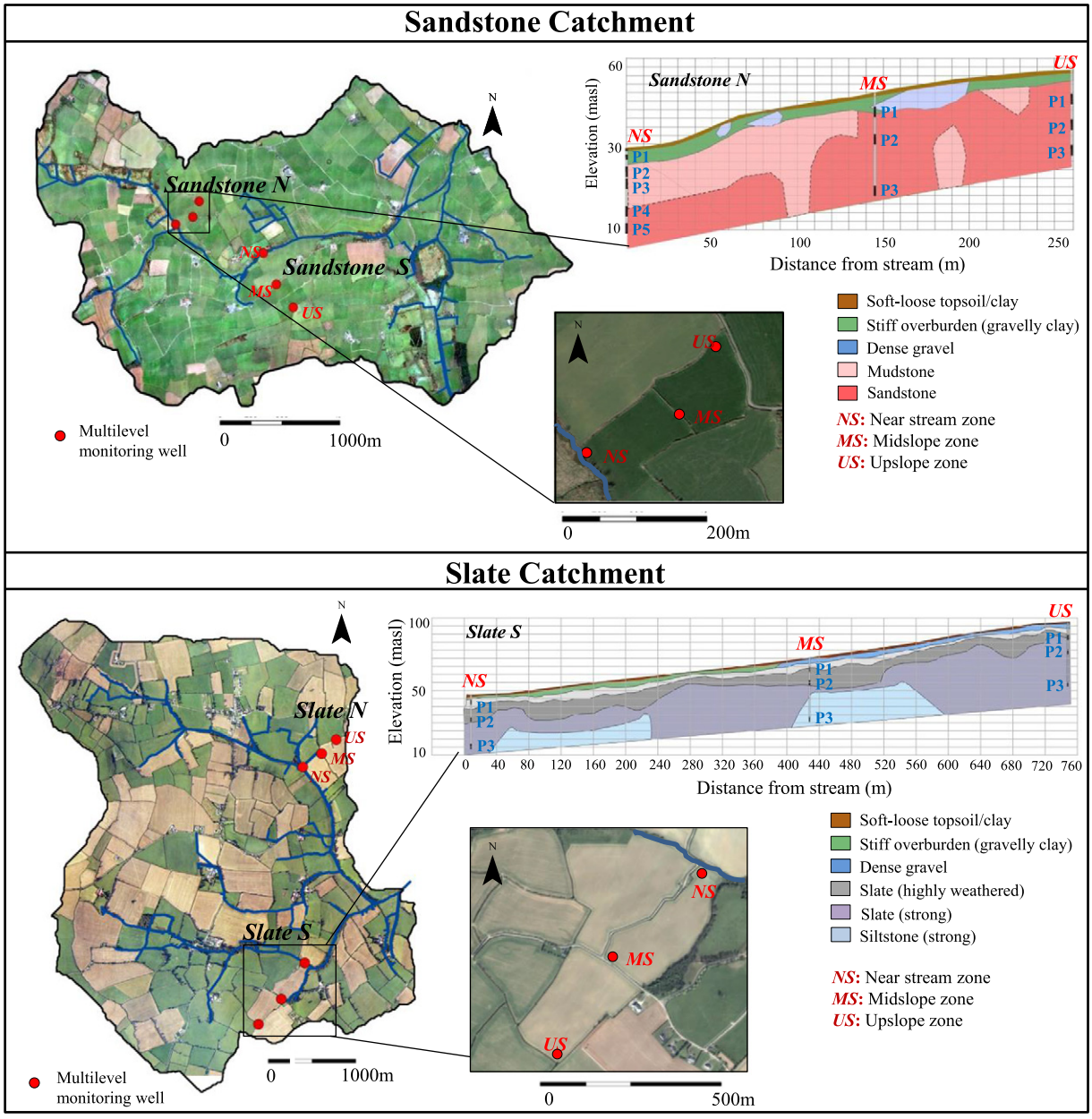

Fig. 1. Location of experimental catchments, stream network, field boundaries and instrumented hillslopes. Also illustrated are geological cross sections of the *Sandstone N* and *Slate S* hillslopes showing the location of the multilevel monitoring wells. Note P1, P2 etc. refers to piezometer screened intervals.

of multilevel monitoring wells at the *Sandstone N* and *Slate S* hillslopes. The length and depth of each piezometer screened intervals and hillslope hydraulic properties are presented in Table 1.

2.3. Hillslope characterisation

At the sandstone hillslopes, Quaternary deposits are dominated by free draining loam to clay loam underlain by layers of dense gravel and gravelly clay with weathered mudstone. Bedrock consists of a complex 3 dimensional pattern of mudstone and sandstone with minor siltstone and exhibits varying degrees of weathering (Fig. 1, Supplementary Fig. 1b). The aquifer is characterised as unconfined (GSI, 2016) and exhibits a high baseflow index (BFI) of 73% (mean: 2012–13). BFI describes the proportion of flow in a stream which is supplemented by groundwater discharge and was calculated after Mellander et al. (2012). In situ measurements of Ksat at both hillslopes indicated a layered distribution of permeability (Table 1), becoming less permeable with depth.

The slate hillslopes are characterised by clay to clay loam underlain by dense gravel and firm gravelly clay layers. An extensive zone of highly weathered to moderately weathered slate bedrock is apparent at both hillslope sites. In *Slate N*, the weathered zone ranges in thickness from approximately 4 to 11 m BGL, increasing in magnitude towards the bottom of the hillslope (Supplementary Fig. 2a). In *Slate S*, the weathered zone is more extensive, ranging in thickness from 5 to 18 m BGL, with greatest magnitudes in midslope and near stream zones (Fig. 1). Underlying the weathered zone is competent slate and siltstone bedrock, showing evidence of localised fracturing. The aquifer in the slate catchment is unconfined (GSI, 2016) with a BFI of 77% (mean: 2013–15), indicating that up-gradient groundwater hydrogeochemistry has a significant effect on stream water quality. The distribution of Ksat revealed that *Slate N* and *Slate S* are highly permeable (Table 1), owing to the density and vertical extent of bedrock fracturing. A comprehensive description of hillslope geology and aquifer properties is provided in Supplementary Section 1.

2.4. Water sampling

Groundwater sampling was carried out on a monthly basis from July 2013 until May 2015. Samples were collected from the centre of each well screen using a 200 mL double valve bailer (Solinst, Canada). Stream and drain samples were collected simultaneously with groundwater samples. Samples for nitrogen components (NO_3^-, NO_2^-, NH_4^+),Cl^-, reduced metals (Fe^{2+} & Mn^{2+}) and dissolved organic carbon (DOC) were filtered in-situ through a 0.45 μm hydrophilic membrane filter into polypropylene sample tubes (50 mL). Groundwater temperature, pH, electrical conductivity, redox potential (Eh) and dissolved oxygen (DO) were simultaneously measured using an in-situ multi-parameter (Aquameter) probe. Seasonal groundwater dissolved gas sampling (N_2, N_2O and DO) was undertaken to complement the monthly hydrogeochemical dataset. Samples for N_2, Argon (Ar) and DO were collected by overflowing groundwater into 12 mL exetainers (Labco Ltd., Wycombe, UK), while groundwater N_2O samples were overflowed into 160 mL glass serum bottles. All gaseous samples were immediately sealed following collection and stored under water (at 4 °C) prior to analysis.

2.5. Hydrochemistry

Total oxidised nitrogen (NO_3^- & NO_2^-), NO_2^-, Cl^-, NH_4^+ were analysed by Aquakem 600 Discrete Analyser (Aquakem 600A, 01621 Vantaa, Finland) following the hydrazine reduction, sulphanilamide diazotisation and dichloroisocyanurate hydrolysis methods respectively. Groundwater NO_3^- was calculated by subtracting NO_2^- from total oxidised nitrogen. DOC and total N were analysed by catalytic combustion using a Shimadzu TOC-L analyser (TOC-V cph/cpn: Shimadzu Corporation, Kyoto, Japan). Reduced metals (Fe^{2+} & Mn^{2+}) were analysed by inductively coupled plasma emission spectrometry (Agilent 5100 + Agilent Technologies, 5301 Stevens Creek Blvd, Santa Clara, CA 95051, United States). Total N_2, DO and Argon (Ar) were analysed using membrane inlet mass spectrometry (MIMS), according to the average

Table 1
Length and depth of piezometer screened intervals, hillslope permeability (Ksat) and hillslope piezometric levels.

Sandstone catchment						Slate catchment					
*Hillslope Zone	Piezometric water level (m BGL)	*Well screen		*Ksat		*Hillslope Zone	Piezometric water level (m BGL)	*Well screen		*Ksat	
		Subsoil/ weathered rock	Bedrock	Subsoil/ weathered rock	Bedrock			Subsoil/ weathered rock	Bedrock	Subsoil/ weathered rock	Bedrock
Sandstone N (NS)	Min: 0.0 Max: 0.7	P1: 2-3.5 P2: 5.5-8.5	P3: 9-12 P4: 16.5-19.5 P5: 22-25	P1: 2.8 P2: 0.8	P3: 0.6 P4: 0.7 P5: 0.3	*Slate N* (NS)	Min: 0.0 Max: 2.5	P1: 1-4 P2: 9-13	P3: 32-52	P1: 1.2 P2: 0.5	P3: 0.08
Sandstone N (MS)	Min: 0.1 Max: 4.0	P1:4-7	P2: 12-15 P3: 27-30	P1: 2.5	P2: 0.4 P3: 0.3	*Slate N* (MS)	Min: 0.0 Max: 3.9	P1: 1-4	P2: 25-28 P3: 37-40	P1: 2.2	P2: 1.3 P3: 0.15
Sandstone N (US)	Min: 1.1 Max: 7.0		P1: 7-10 P2: 14.5-17.5 P3: 22-25		P1: 1.0 P2: 1.9 P3: 0.09	*Slate N* (US)	Min: 3.0 Max 11.4		P1: 12-15 P2: 27-30		P1: 1.03 P2: 1.4
Sandstone S (NS)	Min: 0.1 Max: 0.5	P1: 4-7	P2: 10-13 P3: 17-20	P1: 0.53	P2: 0.99 P3: 0.35	*Slate S* (NS)	Min: 0.1 Max: 1.0	P1: 3.5-6.5	P2: 14-17 P3: 30.5-33.5	P1: 4.2	P2: 5.2 P3: 0.4
Sandstone S (MS)	Min: 1.2 Max: 12.7		P1: 10.5-13.5 P2: 17-20 P3: 27-30		P1: 2.8 P2: 0.98 P3: 0.54	*Slate S* (MS)	Min: 3.0 Max: 9.8		P1: 10.5-13.5 P2: 17-20 P3: 27-30		P1: 4.2 P2: 4.0 P3: 0.9
Sandstone S (US)	Min: 5.6 Max: 14.0		P1: 13-16 P2: 27-30		P1: 0.40 P2: 0.403	*Slate S* (US)	Min: 6.3 Max: 10.6	P1: 7-11	P2: 16-19 P3: 37-40	P1: n.d	P2: 1.0 P3: 5.3

*Hillslope zone: NS = near stream, MS = midslope, US = upslope.
*Well screen: metres below ground level of the top and bottom of each screened interval.
*Ksat: Hydraulic conductivity (m/day) calculated after Bower and Rice (1976).

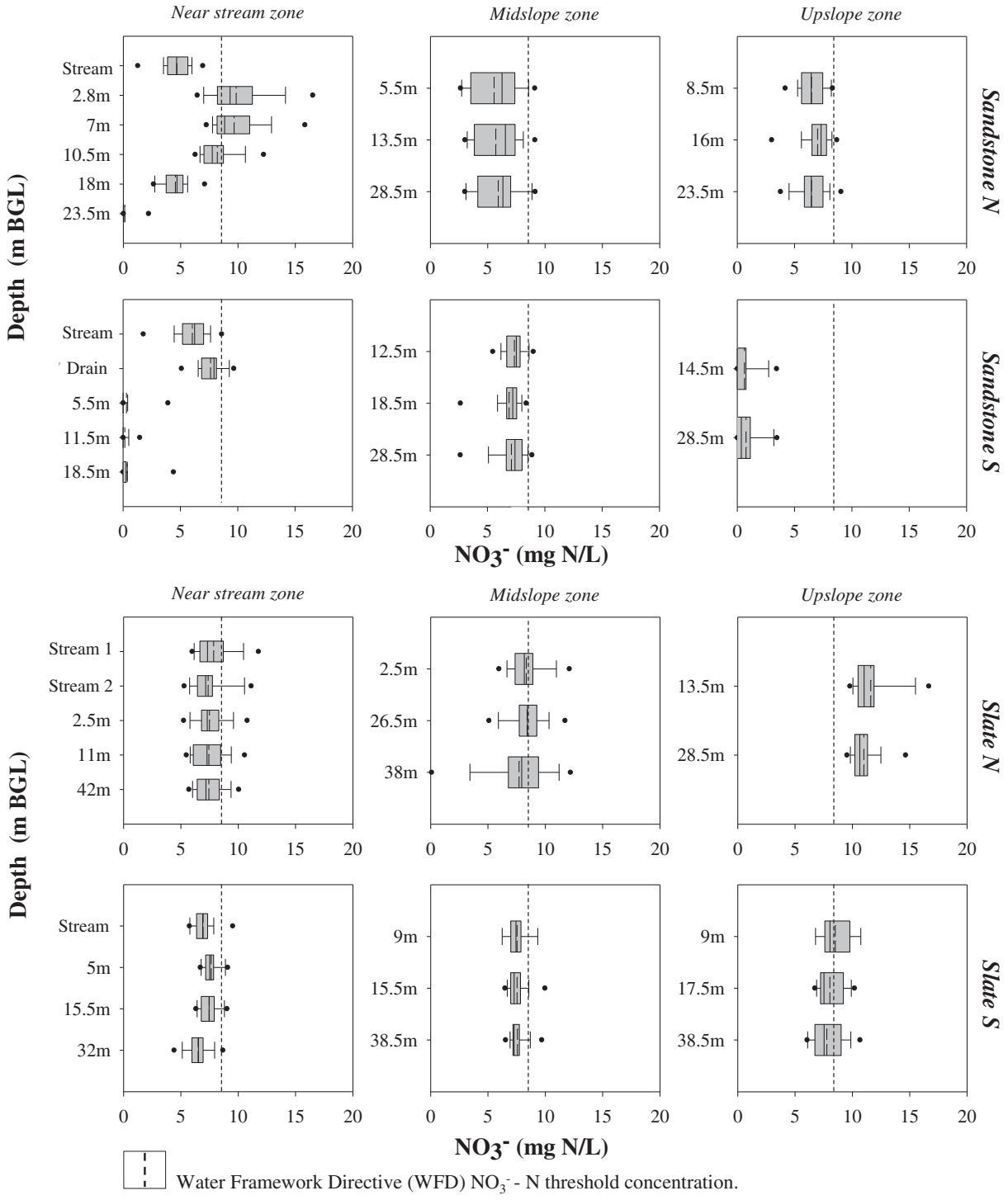

Fig. 2. Boxplots of groundwater and stream NO_3^- from 2013 to 2015 in the sandstone and slate catchments, arranged by hillslope, slope position, and piezometer sampling depth.

recharge temperature during sampling (Kana et al., 1994). Denitrified N_2, termed excess N_2 hereafter, was calculated after Weymann et al. (2008) using the ratio of N_2/Ar in groundwater and temperature based solubility constants. Preparation of groundwater N_2O samples was carried out using the headspace extraction technique according to the methodology outlined in Jahangir et al. (2012b). The N_2O concentration of the extracted headspace gas was analysed using electron capture gas chromatography (CP-3800, Varian, Inc. USA). Frozen samples for natural abundance stable isotopes were packed in dry ice and shipped to the UC Davis Stable Isotope Facility, University of California, USA for analysis. Samples for $\delta^{15}N_{NO3}$, $\delta^{18}O_{NO3}$ and $\delta^{15}N_{N2O}$ were analysed using the bacterial denitrifier method (Sigman et al., 2001).

2.6. Total initial nitrogen (N_{INI}), denitrification reaction progress (RP), groundwater N_2O emission factors ($EF_{5g}1$ & $EF_{5g}2$) and FracLEACH

It is assumed that denitrification along a groundwater flow path results in the reduction of NO_3^- and the production of dissolved N gases. As such, the initial nitrogen concentration (N_{INI}) is calculated as the sum of residual N substrates and accumulated N products (Jahangir

et al., 2013) where:

$$(N_{INI}) = NO_3{}^- - N + NH_4{}^+ - N + NO_2{}^- - N + \text{organic N} + \text{excess } N_2 - N + N_2O - N \quad (1)$$

Reaction progress (RP) is the ratio between products of a given process and starting substrates (Weymann et al., 2008). RP was used to estimate groundwater denitrification using the following relationship:

$$(RP) = (\text{excess } N_2 - N + N_2O - N)/N_{INI} \quad (2)$$

Indirect emissions of N_2O from groundwater were quantified using two methods. The first, termed $EF_{5g}1$ was adopted from Weymann et al. (2008) and takes into account transformations of NO_3^- and N_2O within the aquifer (Eq. (3)). The second $EF_{5g}2$ has been adopted by the IPCC (2006), typically in studies lacking gaseous N data, and assumes no further transformation of NO_3^- and N_2O that has been leached to groundwater (Eq. (4)).

$$EF_{5g}1 = N_2O - N/N_{INI} - N \quad (3)$$

$$EF_{5g}2 = N_2O - N/NO_3^- - N \quad (4)$$

FracLEACH describes the quantity of dissolved N leached from soil to groundwater as a proportion of the total N load applied via agricultural practises. FracLEACH was quantified using the following relationship:

$$\text{FracLEACH } (\%) = Q_{GW}(m^3/ha/yr.) * NO_3{}^- - N_s\left(\text{kg N}/m^3\right) / \text{Total N input (kg N/ha/yr.)} \quad (5)$$

Q_{GW} represents groundwater discharge and was calculated as Q_{EF} (m^3/Ha) * baseflow index (BFI). Q_{EF} refers to total recharge, measured as effective rainfall (m/yr.) multiplied by field area (ha). Effective rainfall was calculated by subtracting potential evapotranspiration (calculated according to Penman-Monteith) from total rainfall. Total recharge multiplied by the BFI was assumed to equal groundwater discharge. Groundwater discharge was multiplied by NO_3^-–N in the shallow groundwater of each hillslope (NO_3^-–N_s) providing a total load of NO_3^-–N per year. Wells exhibiting aerobic conditions were chosen for the FracLEACH calculation to negate the confounding effect of attenuation on leaching rates. Dividing the total load of NO_3^-–N_s by the total load of N applied provided a measurement of FracLEACH. The total load of organic and inorganic N applied was calculated from detailed farmer records specific to each hillslope field (2012 — 2013). Hillslope landuse, applied N, values of FracLEACH and the total loads of NO_3^-–N_s for each study hillslope are provided in Table 2.

2.7. Statistical analysis

In order to identify statistically significant relationships ($p < 0.05$) between parameters, a correlation analysis between influential hydrological, hydrogeological and hydrogeochemical variables and NO_3^-, N_2O and excess N_2 was undertaken. The Pearson product moment approach was utilised when data were approximately normally distributed, with appropriate transformation and rescaling of the data where non-normality was apparent. Where it was not possible to transform data to normality, the Spearman rank approach was used. A repeated measures mixed ANOVA analysis (SAS, 2009), including covariance modelling for effects across sampling dates, was used to identify the significant effects of spatial parameters, including sampling depth and hillslope zone on groundwater hydrogeochemistry. The effect of groundwater sampling depth and groundwater residence times on groundwater hydrogeochemistry has been examined in several studies (Jahangir et al., 2012a; Fenton et al., 2009; Weymann et al., 2008). Typically aquifer permeability decreases with increasing depth (Jahangir et al., 2012a), while groundwater residence times increase (Fenton et al., 2011). The use of depth as a grouping factor provides insight into these hypotheses. Each hillslope was split into three zones: near stream, midslope and upslope zone. The depth of the unsaturated zone has been identified as a dominant controlling factor on groundwater nitrate concentrations (Spalding and Exner, 1993). In the near stream zone, the water table is close to the surface. In the midslope and upslope zones, the depth to the water table and depth of the unsaturated zone increases, with greatest thickness in the upslope zone. The statistical model also accounted for between catchment variability (sandstone vs. slate), and within catchment variability e.g. *Sandstone N* vs. *Sandstone S*. Given the extensive range of sampling depths across catchments, depth was grouped into six categories namely 0–5, 5–10, 10–15 15–20, 20–30 and >30 m BGL. The interactions between categorical variables were also scrutinised within the model, while a validation of the model assumptions was achieved using a residual analysis.

3. Results

3.1. NO_3^-, NH_4^+ and NO_2^- concentrations

The spatial distribution of groundwater and stream NO_3^- in the sandstone and slate catchments, organised by hillslope, hillslope zone and sample depth are illustrated in Fig. 2. Mean groundwater NO_3^- concentration was lower ($p < 0.001$) in the sandstone catchment (4.9 mg N/L) compared to the slate catchment (8.1 mg N/L). This pattern was echoed in stream concentrations with NO_3^- in the slate catchment streams (mean: 7.3 mg N/L) exceeding the sandstone streams (mean: 5.4 mg N/L) by 32% ($p < 0.001$).

The coefficient of variation (CV) was used as a measure of spatial variability specific to each experimental hillslope, calculated using the overall hillslope mean, and standard deviation from the mean at each spatial sampling interval. A high CV value indicates spatial heterogeneity of a given parameter associated with different sampling depths and hillslope zones i.e. upslope vs. midslope vs near stream. A low CV indicates spatial uniformity. The spatial distribution of groundwater NO_3^- in the sandstone catchment was complex (CV *Sandstone N*: 42% vs. *Sandstone S*: 117%). Significant relationships were identified between hillslopes ($p < 0.0001$) and sample depths ($p < 0.05$), with significant

Table 2
Hillslope landuse, surface applied N, N leached to groundwater and FracLEACH.

Sandstone catchment					Slate catchment				
Hillslope	Landuse	*Applied N (kg N/ha/yr.)	*NO_3^-–N_s (kg N/ha/yr.)	FracLEACH (%)	Hillslope	Landuse	*Applied N	*NO_3^-–N_s (kg N/ha/yr.)	FracLEACH (%)
Sandstone N	Grassland, dairy production	Inorganic: 295.3 Organic: 0	39.1	14	*Slate N*	Arable, spring barley production.	Inorganic: 122.0 Organic: 21.0	69.0	41
Sandstone S	Grassland, dairy production	Inorganic: 301.5 Organic: 78.6	72.5	21	*Slate S*	Arable, spring barley production.	Inorganic:154.8 Organic: 0	62.4	44

*Applied N: Mean applications of inorganic and organic N (2012–2013).
*$NO_{3\_}$—Ns: Mean load of $NO_{3\_}$ leached to shallow groundwater (2012–2013).

interactions between hillslope and hillslope zone ($p < 0.001$), hillslope and depth ($p < 0.05$) and hillslope zone and depth ($p < 0.0001$). An analysis of the slope of the interaction terms indicated that depth had a greater effect on NO_3^- concentration in *Sandstone N* vs. *Sandstone S*, while in both hillslopes, a combination of near stream hillslope zone and depth had the greatest baring on groundwater NO_3^- concentrations. In *Sandstone N*, a negative correlation was observed between depth and NO_3^- concentration. In the near stream zone, there was a clear concentration gradient in NO_3^- moving deeper down the depth profile (Fig. 3a). The gradient in NO_3^- concentration mirrored the distribution

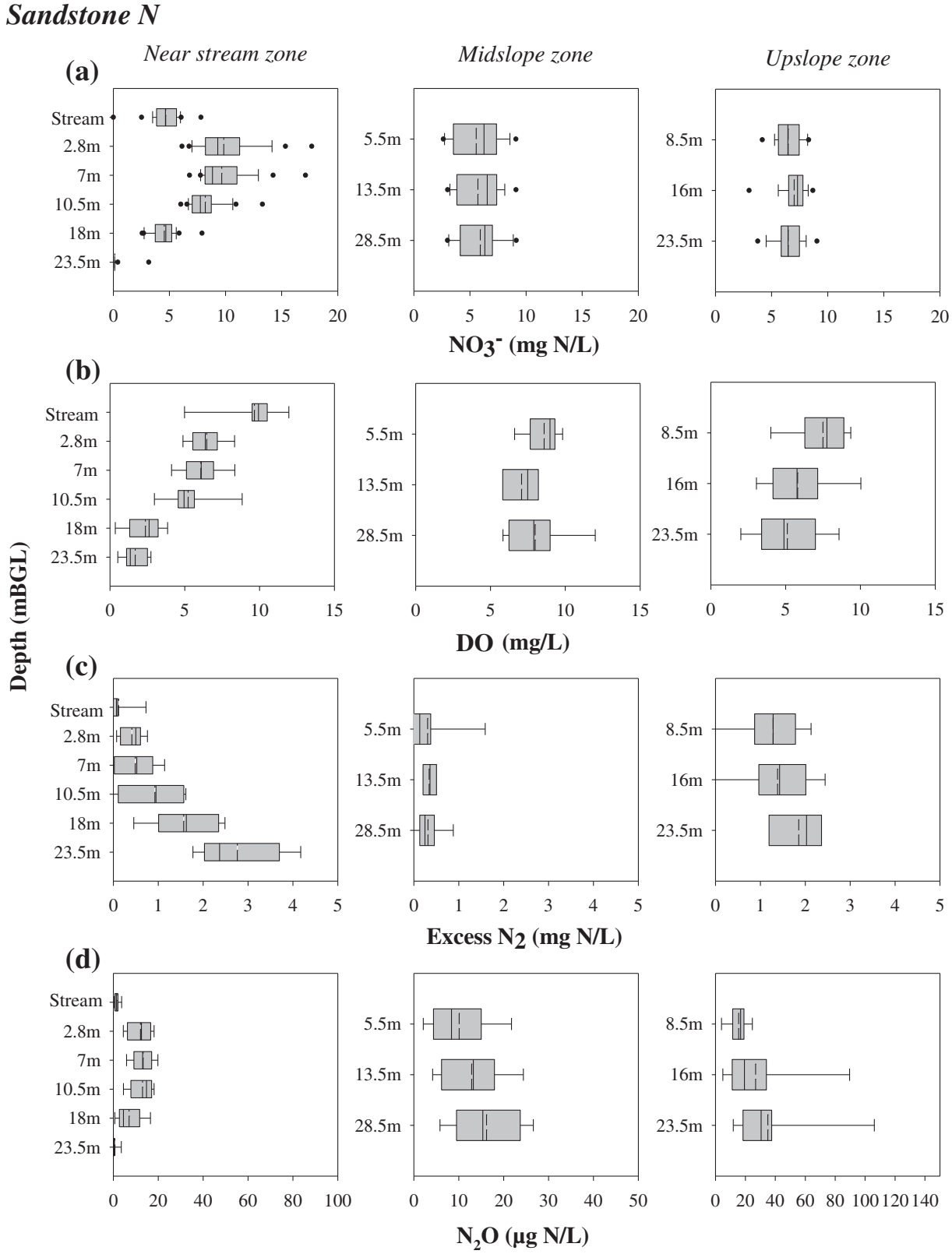

Fig. 3. Boxplots of groundwater and stream NO_3 –, DO, excess N_2 and N_2O from 2013 to 15 in *Sandstone N*, arranged by slope position and piezometer sampling depth.

of groundwater DO (Fig. 3b). NO_3^- concentrations in the near stream zone were significantly lower than the midslope ($p < 0.001$) and upslope ($p < 0.005$) zones. Despite elevated NO_3^- concentrations in the near stream shallow groundwater of *Sandstone N* (mean 9.8 mg N/L between 2 and 8.5 m BGL), stream concentrations were significantly lower (mean 4.6 mg N/L), most closely reflecting deeper groundwater. In *Sandstone S*, groundwater NO_3^- in the near stream zone was lower than the midslope zone ($p < 0.0001$), showing no significant difference with the upslope zone. At all sample depths in the near stream and upslope zones, groundwater NO_3^- was either below or marginally exceeded the limit of detection (0.25 mg N/L) (Fig. 2). Fig. 4a and b illustrate the relationship between NO_3^- and hydraulic conductivity (Ksat) and NO_3^- and the water table ratio. The water level ratio refers the ratio between the depth of the unsaturated zone and the total depth of sampling. The nearer the ratio is to 1, the closer the water table is to the ground surface. The ratio also takes the depth of the saturated water column into account. Therefore the greater the depth of the overlying water column, the closer the ratio is to 1. Water level ratios are highest where a deep well has a shallow water table. In the sandstone catchment, groundwater NO_3^- increased significantly with increasing Ksat values ($r = 0.54, p < 0.05$) and decreased significantly with increasing water table ratios ($r = 0.58, p < 0.05$). Typically, Ksat decreased with increasing depth BGL corresponding to less weathered bedrock, while the water level ratio decreased moving upslope corresponding to increases in the depth of the unsaturated zone. Stream NO_3^- in *Sandstone S* was significantly higher ($p < 0.05$) than the *Sandstone N*. The mean stream concentration of 6.0 mg N/L closely reflected midslope groundwater and water sampled from an upstream tile drain.

In the slate catchment, there was a significant interaction between hillslope and hillslope zone ($p < 0.0001$). As such, while there was a clear effect of hillslope zone on NO_3^- concentration, the effect was specific to each hillslope. *Slate N* exhibited higher groundwater NO_3^- than *Slate S* with mean concentrations of 8.7 and 7.6 mg N/L respectively. *Slate S* was characterised by spatial uniformity throughout the hillslope (CV: 6.9%) with no significant differences identified as a function of hillslope zone or sampling depth (Fig. 2). In *Slate N*, there was greater spatial variation than *Slate S* (CV: 18.9%) with a hillslope zone effect ($p < 0.0001$). Highest NO_3^- concentrations occurred in the upslope zone, with lower concentrations in the midslope and near stream zones. In the slate catchment, no significant relationships were identified between NO_3^- and Ksat or NO_3^- and water table ratio (Fig. 4). In both slate hillslopes, stream NO_3^- concentrations were similar to shallow groundwater.

Groundwater NH_4^+ concentrations where marginally lower in sandstone catchment compared to the slate catchment (mean sandstone: 0.03 mg N/L, mean slate: 0.04 mg N/L). In the sandstone catchment there were no significant differences between hillslopes means, with limited spatial variability (CV: 13%). Similarly, in the slate catchment, no significant relationships were identified between hillslopes with limited spatial variation across hillslope zones and sample depths (CV: 25%). Groundwater NO_2^- concentrations were typically either at or below the limits of detection (0.006 mg N/L) with mean concentrations of 0.002 and 0.007 mg N/L in the slate and sandstone catchments.

3.2. Groundwater hydrochemistry

3.2.1. Aquifer aerobicity

Groundwater DO was lower (ANOVA; $p < 0.001$) in the sandstone catchment compared to the slate catchment (mean sandstone: 5.5 vs. mean slate: 8.9 mg/L). In the sandstone catchment, mean DO concentrations were 5.8 and 4.1 mg/L in *Sandstone N* and *Sandstone S*, respectively. Spatial variation was high in both hillslopes (CV *Sandstone N*: 38% vs. CV *Sandstone S*: 54%) and there was a significant effect of sampling depth ($p < 0.01$) and hillslope zone ($p < 0.0001$) on groundwater DO. In both hillslopes, near stream zones had the lowest DO ($p < 0.0001$) with the exception of the upslope monitoring well in *Sandstone S*, which showed comparably low concentrations (Table 3). DO typically decreased with increasing depth, while a distinct geochemical gradient was apparent in the near stream zone of *Sandstone N* (Table 3). The sandstone catchment was characterised by anaerobic conditions at a number of spatial sampling points. Screened intervals with DO <3 mg/L included the near stream zones of *Sandstone N* (18.5 and 23.5 m BGL) and *Sandstone S* (5.5, 11.5 and 18.5 m BGL) and the upslope zone of *Sandstone S* (14.5 m BGL). Fig. 4c and d illustrate the relationship between DO and hydraulic conductivity (Ksat) and DO and the water table ratio (as described in Table 1). In the sandstone catchment, groundwater DO

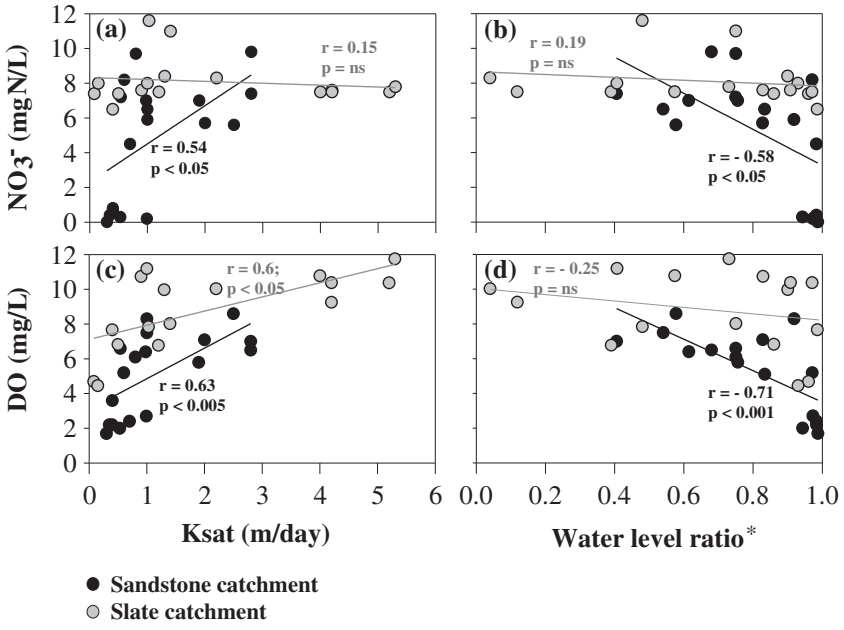

Fig. 4. a & b Linear regression analysis of hydraulic conductivity (Ksat) and water level ratio vs. NO3 — in the sandstone and slate catchments. (Fig. 4c & 4d) Regression analysis of hydraulic conductivity (Ksat) and water level ratio vs. DO in the sandstone and slate catchments. $P < 0.05$ = significant correlation; ns = not significant. Black regression line = sandstone catchment. Grey regression line = slate. Note: water level ratio* refers to the depth of the water table BGL, relative to the total depth of the well screen BGL.

Table 3
Mean groundwater and stream NO_3^- (± standard error SE) vs. aerobicity, bacterial energy sources, denitrification reaction products and N_2O emissions arranged by hillslope, hillslope positions and piezometric sampling depth in the sandstone catchment.

Hillslope zone*/ Depth* (m BGL)	Reactive N			Aerobicity		Bacterial energy sources			Denitrification rate & products			N_2O emissions
	NO_3^- (mg N/L)	N_{INI}* (mg N/L)	NO_3^-/Cl^- (ratio)	DO (mg/L)	Eh (mV)	DOC (mg/L)	Fe^{2+} (μg/L)	Mn^{2+} (μg/L)	RP*	excess N_2 (mg N/L)	N_2O (μg N/L)	N_2O–$EF_{5g}1$* Above IPCC 2006: ✓, below: ✘
Sandstone N												
Stream	4.7 (0.3)	5.5 (0.4)	0.16 (0.01)	9.6 (0.7)	94.9 (11.8)	6.3 (1.4)	18.0 (3.3)	11.6 (2.9)	0.02 (0.02)	0.1 (0.1)	1.5 (0.4)	0.0003 (0.0001) ✘
NS (2.8 m)	9.8 (0.5)	12.5 (1.0)	0.35 (0.01)	6.5 (0.4)	65.6 (7.3)	2.0 (0.2)	10.5 (6.8)	6.2 (1.3)	0.04 (0.01)	0.4 (0.1)	12.1 (1.8)	0.0010 (0.0001) ✘
NS (7 m)	9.7 (0.4)	12.1 (0.9)	0.35 (0.01)	6.1 (0.5)	62.9 (11.3)	2.0 (0.3)	5.7 (2.1)	6.6 (1.7)	0.04 (0.01)	0.5 (0.2)	13.3 (1.6)	0.0011 (0.0002) ✘
NS (10.5 m)	8.2 (0.3)	10.1 (0.8)	0.30 (0.01)	5.2 (0.7)	39.5 (12.2)	1.9 (0.4)	4.7 (2.1)	11.6 (2.6)	0.09 (0.02)	0.9 (0.2)	13.0 (1.8)	0.0013 (0.0002) ✘
NS (18 m)	4.5 (0.2)	6.5 (0.4	0.17 (0.01)	2.4 (0.8)	−21.2 (16.1)	1.9 (0.3)	3.4 (1.1)	54.6 (14.9)	0.25 (0.03)	1.6 (0.2)	7.1 (1.9)	0.0010 (0.0002) ✘
NS (23.5 m)	0.0 (0.02)	3.0 (0.3)	0.01 (0.00)	1.7 (0.6)	−73.7 (30.0)	2.5 (0.9)	79.3 (28.0)	633.2 (64.2)	0.95 (0.01	2.9 (0.3)	0.7 (0.4)	0.0002 (0.0001) ✘
MS (5.5 m)	5.6 (0.4)	7.4 (0.6	0.23 (0.01)	8.6 (0.4)	107.4 (7.8)	2.6 (0.3)	3.2 (1.3)	4.0 (0.9)	0.05 (0.03)	0.3 (0.2)	10.1 (2.2)	0.0014 (0.0003) ✘
MS (13.5 m)	5.7 (0.4)	7.6 (0.6)	0.24 (0.01)	7.1 (0.5)	102.0 (8.9)	2.9 (0.3)	4.1 (1.9)	12.5 (9.4)	0.05 (0.01)	0.3 (0.1)	12.9 (2.3)	0.0017 (0.0003) ✘
MS (28.5 m)	5.9 (0.4)	7.6 (0.7)	0.24 (0.01)	8.3 (0.9)	120.1 (15.4)	2.7 (0.3)	15.7 (12.2)	6.1 (1.3)	0.04 (0.01)	0.3 (0.1)	16.2 (2.5)	0.0022 (0.0003) ✘
US (8.5 m)	6.5 (0.2)	8.3 (0.5)	0.28 (0.01)	7.5 (0.6)	120.7 (9.6)	2.7 (0.6)	6.8 (3.8)	3.1 (0.5)	0.16 (0.03)	1.3 (0.2)	15.5 (2.0)	0.0019 (0.0003) ✘
US (16 m)	7.0 (0.3)	8.9 (0.5)	0.27 (0.01)	5.8 (0.9)	117.2 (9.6)	2.6 (0.5)	3.4 (1.5)	14.0 (6.8)	0.18 (0.02)	1.6 (0.2)	26.8 (8.6)	0.0038 (0.0016) ✓
US (23.5)	6.5 (0.3)	8.6 (0.4)	0.26 (0.01)	5.1 (2.2)	123.4 (12.1)	2.4 (0.5)	18.9 (14.6)	16.2 (11.4)	0.23 (0.03)	1.9 (0.2)	35.0 (9.4)	0.0047 (0.0015) ✓
Sandstone S												
Stream	6.0 (0.3)	7.1 (0.4)	0.19 (0.01)	8.7 (0.7)	99.5 (11.4)	6.6 (1.4)	22.5 (5.1)	15.1 (2.9)	0.03 (0.02)	0.2 (0.1)	5.4 (1.3)	0.0008 (0.0002) ✘
NS (5.5 m)	0.3 (0.2)	2.6 (0.5)	0.02 (0.008)	2.0 (1.4)	18.4 (19.8)	2.1 (0.8)	2910.3 (484.7)	2997.3 (210.1)	0.88 (0.05)	2.4 (0.5)	1.1 (0.8)	0.0004 (0.0002) ✘
NS (11.5 m)	0.2 (0.1)	2.4 (0.4)	0.01 (0.002)	2.7 (1.0)	20.1 (11.7)	1.9 (0.6)	2111.6 (422.6)	2407.0 (295.6)	0.89 (0.03)	2.2 (0.4)	1.0 (0.4)	0.0005 (0.0002) ✘
NS (18.5 m)	0.4 (0.3)	2.7 (0.5)	0.02 (0.01)	2.2 (1.2)	20.9 (20.1)	1.9 (0.6)	2560.1 (394.6)	1860.9 (135.1)	0.89 (0.02)	2.4 (0.4)	1.4 (0.9)	0.0016 (0.0014) ✘
MS (12.5 m)	7.4 (0.2)	9.7 (0.7)	0.27 (0.007)	7.0 (0.5)	58.9 (6.7)	3.5 (1.7)	6.7 (2.1)	11.2 (4.1)	0.16 (0.03)	1.7 (0.5)	21.6 (4.4)	0.0023 (0.0004) ✘
MS (18.5 m)	7.0 (0.3)	9.4 (0.9)	0.24 (0.01)	6.4 (0.5)	52.5 (21.9)	2.6 (1.2)	8.4 (3.0)	14.7 (3.8)	0.18 (0.03)	1.8 (0.5)	20.3 (4.2)	0.0021 (0.0005) ✘
MS (28.5 m)	7.2 (0.3)	9.2 (1.2)	0.26 (0.01)	6.6 (0.9)	56.3 (29.2)	2.6 (0.9)	61.9 (26.0)	89.5 (31.1)	0.17 (0.04)	1.6 (0.4)	22.8 (5.0)	0.0025 (0.0005) ✓
US (14.5 m)	0.6 (0.2)	4.4 (1.1)	0.03 (0.008)	2.2 (1.2)	23.7 (11.5)	2.0 (0.5)	2910.2 (765.0)	2061.3 (180.1)	0.82 (0.07)	3.4 (0.8)	4.9 (2.4)	0.0015 (0.0005) ✘
US (28.5 m)	0.8 (0.2)	4.8 (0.9)	0.03 (0.007	3.6 (1.9)	29.8 (22.1)	3.8 (2.5)	1425.0 (469.7)	1691.4 (177.9)	0.73 (0.07)	3.3 (0.8)	7.1 (4.6)	0.0013 (0.0005) ✘

Hillslope zone *: NS = near stream, MS = midslope, US = upslope. Depth*: metres below ground level to the centre of each well screen.
N_{INI}*: $NO_3^- + NH_4^+ + NO_2^-$ + organic N + excess N_2 + N_2O.
Reaction progress (RP)*: excess N_2 + N_2O/N_{INI}.
$EF_{5g}1$*: IPCC N_2O emission factor: N_2O/N_{INI}.

Table 4
Mean groundwater and stream NO_3^- (± standard error SE) vs. aerobicity, bacterial energy sources, denitrification reaction products and N_2O emissions arranged by hillslope, hillslope positions and piezometric sampling depth in the slate catchment.

Hillslope zone*/ Depth* (m BGL)	Reactive N			Aerobicity		Bacterial energy sources			Denitrification rate & products			N_2O emissions
	NO_3^- (mg N/L)	N_{INI}^* (mg N/L)	NO_3^-/Cl^- (Ratio)	DO (mg/L)	Eh (mV)	DOC (mg/L)	Fe^{2+} (μg/L)	Mn^{2+} (μg/L)	RP*	Excess N_2 (mg N/L)	N_2O (μg N/l)	N_2O–$EF_{5g}1$* Above IPCC 2006: ✓, below:✘
Slate N												
Stream I	7.8 (0.2)	8.7 (0.8)	0.41 (0.01)	10.56 (0.3)	110.6 (8.0)	2.5 (0.6)	14.6 (4.9)	4.0 (1.4)	0.00 (0.11)	0.02 (0.5)	0.69 (0.5)	0.0001 (0.00008) ✘
Stream II	7.4 (0.2)	8.9 (1.0)	0.40 (0.02)	9.93 (0.6)	111.2 (7.2)	2.3 (0.6)	16.9 (5.6)	3.6 (1.2)	0.01 (0.01)	0.10 (0.1)	0.56 (0.1)	0.0001 (0.00001) ✘
NS (2.5 m)	7.5 (0.2)	10.8 (0.9)	0.37 (0.02)	6.78 (1.2)	139.8 (10.5)	2.0 (0.8)	27.3 (5.9)	13.1 (2.8)	0.09 (0.02)	0.87 (0.1)	6.57 (1.8)	0.0006 (0.0002) ✘
NS (11 m)	7.4 (0.2)	9.4 (0.9)	0.38 (0.02)	6.83 (1.1)	139.6 (9.3)	1.7 (0.6)	21.1 (7.3)	14.7 (4.5)	0.08 (0.02)	0.73 (0.1)	5.89 (1.8)	0.0006 (0.0001) ✘
NS (42 m)	7.4 (0.2)	8.9 (0.8)	0.37 (0.02)	4.69 (1.2)	128.0 (10.7)	1.7 (0.6)	12.7 (4.4)	12.7 (9.1)	0.06 (0.02)	0.62 (0.2)	6.30 (1.8)	0.0007 (0.0001) ✘
MS (2.5 m)	8.3 (0.2)	9.6 (0.9)	0.39 (0.01)	10.03 (0.7)	119.8 (15.2)	1.9 (0.8)	11.0 (3.1)	21.8 (8.5)	0.06 (0.03)	0.68 (0.3)	1.78 (1.5)	0.0002 (0.0002) ✘
MS (26.5 m)	8.4 (0.2)	8.6 (0.8)	0.40 (0.02)	9.98 (0.5)	131.9 (9.5)	1.7 (0.6)	6.9 (2.2)	24.0 (11.7)	0.10 (0.03)	0.76 (0.3)	1.39 (0.3)	0.0001 (0.00003) ✘
MS (38 m)	8.0 (0.3)	7.3 (0.5)	0.37 (0.02)	4.45 (1.1)	126.9 (9.9)	2.0 (0.6)	9.9 (2.9)	19.8 (9.3)	0.32 (0.13)	2.50 (0.7)	3.56 (0.9)	0.0004 (0.0001) ✘
US (13.5 m)	11.6 (0.2)	13.57 (1.3)	0.46 (0.01)	7.85 (0.8)	150.5 (8.7)	2.0 (0.7)	9.7 (3.2)	6.6 (2.9)	0.05 (0.02)	0.86 (0.2)	3.26 (0.6)	0.0002 (0.00004) ✘
US (28.5 m)	11.0 (0.3)	12.46 (0.4)	0.46 (0.02)	8.02 (0.5)	138.8 (9.5)	1.8 (0.7)	13.4 (6.5)	7.2 (3.4)	0.09 (0.02)	1.12 (0.2)	3.43 (0.6)	0.0002 (0.00004) ✘
Slate S												
Stream	6.9 (0.1)	7.3 (0.9)	0.37 (0.01)	10.72 (0.2)	131.5 (8.3)	3.9 (2.4)	27.1 (13.2)	6.1 (3.5)	0.00 (0.02)	0.0 (0.2)	0.7 (0.5)	0.0001 (0.00004) ✘
NS (5 m)	7.6 (0.1)	8.5 (0.3)	0.43 (0.01)	10.38 (0.4)	157.6 (9.7)	1.3 (1.1)	26.7 (3.9)	14.7 (1.7)	0.09 (0.02)	0.8 (0.2)	2.6 (0.5)	0.0003 (0.00005) ✘
NS (15.5 m)	7.5(0.1)	8.2 (0.2)	0.41 (0.01)	10.37 (0.4)	161.4 (9.1)	2.0 (1.1)	8.3 (3.9)	5.0 (1.7)	0.07 (0.02)	0.6 (0.2)	2.5 (0.4)	0.0003 (0.00005) ✘
NS (32 m)	6.5 (0.1)	8.3 (0.8)	0.36 (0.01)	7.67 (0.5)	145.8 (9.1)	0.8 (0.1)	31.6 (15.2)	8.0 (2.6)	0.12 (0.02)	1.1 (0.2)	2.3 (0.4)	0.0003 (0.00005) ✘
MS (9 m)	7.5 (0.2)	7.3 (1.0)	0.48 (0.02)	9.26 (0.4)	149.4 (11.4)	2.3 (1.2)	24.6 (10.6)	3.6 (0.9)	0.02 (0.03)	0.2 (0.3)	13.7 (5.6)	0.0019 (0.0008) ✘
MS (15.5 m)	7.5 (0.1)	7.8 (0.2)	0.47 (0.02)	10.78 (0.2)	163.8 (8.8)	2.4 (1.0)	34.6 (20.4)	7.6 (4.3)	0.03 (0.02)	0.2 (0.1)	2.5 (3.9)	0.0003 (0.0006) ✘
MS (38.5 m)	7.6 (0.1)	8.4 (0.4)	0.47 (0.01)	10.74 (0.6)	155.5 (9.6)	2.0 (1.1)	9.3 (2.3)	4.2 (0.9)	0.07 (0.02)	0.7 (0.2)	2.9 (0.4)	0.0003 (0.00006) ✘
US (9 m)	8.5. (0.4)	11.2 (1.1)	0.55 (0.03)	11.82 (0.1)	161.9 (17.6)	1.3 (0.3)	13.1 (3.0)	7.9 (2.0)	0.07 (0.03)	0.8 (0.4)	3.6 (0.9)	0.0003 (0.00009) ✘
US (17.5 m)	8.0 (0.2)	9.3 (0.8)	0.52 (0.02)	11.20 (0.4)	168.7 (11.3)	1.9 (0.6)	10.6 (3.2)	4.4 (0.8)	0.10 (0.03)	0.9 (0.2)	2.3 (0.6)	0.0002 (0.00007) ✘
US (38.5 m)	7.8 (0.2)	8.7 (0.6)	0.53 (0.02)	11.75 (0.6)	164.7 (9.2)	1.7 (0.7)	17.1 (8.3)	5.9 (1.3)	0.11 (0.03)	1.0 (0.3)	3.4 (0.7)	0.0003 (0.00007) ✘

Hillslope zone *: NS = near stream, MS = midslope, US = upslope. Depth*: metres below ground level to the centre of each well screen.
N_{INI}*: $NO_3^- + NH_4^+ + NO_2^-$ + organic N + excess N_2 + N_2O.
Reaction progress (RP)*: excess N_2 + N_2O/N_{INI}.
$EF_{5g}1$*: IPCC N_2O emission factor.

increased significantly with increasing Ksat values ($r = 0.63$, $p < 0.005$) and decreased significantly with increasing water table ratios ($r = -0.71$, $p < 0.05$).

Within the slate catchment, *Slate N* had lower DO ($p < 0.05$) than *Slate S* with mean values of 7.3 and 10.5 mg/l (Table 4). DO was uniformly high in *Slate S* across groundwater sampling intervals (CV: 12%), whereas *Slate N* exhibited greater spatial variability (CV: 29%). In both hillslopes there existed weakly negative relationships between DO and sampling depth ($p = 0.07$). Groundwater in the slate catchment was consistently aerobic, with limited development of anaerobic zones. A significant positive correlation ($r = 0.6$, $p < 0.05$) was identified between DO and Ksat (Fig. 4c), while no significant relationship was identified between DO and the water table ratio (Fig. 4).

Eh in the sandstone catchment (mean: 54.9 mV) was significantly lower ($p < 0.001$) than the slate catchment (mean: 171.4 mV). Spatial variation was high with CVs of 94% and 50% in *Sandstone N* and *Sandstone S* respectively. Hillslope zone and depth effects mirrored those of DO owing to a strongly positive correlation between Eh and DO ($r = 0.72$; $p < 0.001$) (Table 5). Low Eh (<10 mV) occurred in the near stream zones of *Sandstone N* (18.5 and 23.5 m BGL) and *Sandstone* S (11.5 and 18.5 m BGL) and in the upslope zone of *Sandstone S* (14.5 m BGL) (Table 3). The slate catchment had low spatial variation (CV: 6%) in both hillslopes and elevated Eh (>100 mV) across all hillslope zones and sampling depths.

3.2.2. Bacterial energy sources

Mean groundwater DOC in the sandstone catchment was significantly higher ($p < 0.001$) than the slate catchment (2.5 vs. 1.8 mg/L). In both catchments, stream DOC concentrations were greater than groundwater (mean sandstone: 6.5 vs. mean slate: 2.9 mg/L). In the sandstone catchment, groundwater Mn^{2+} concentrations (mean: 626.3 μg/L) were higher ($p < 0.001$) than the slate site. Within the sandstone catchment, *Sandstone S* had higher Mn^{2+} ($p < 0.05$) than *Sandstone N* with mean concentrations of 1391.7 and 69.8 μg/L respectively (Table 3). In both hillslopes, spatial variability was high (CV *Sandstone N*: 268% vs. *Sandstone S*: 85%). Screened intervals with highest Mn^{2+} (>600 μg/L) were coincident with lowest DO and Eh and included the near stream zones of *Sandstone N* (23.5 m BGL) and *Sandstone S* (5.5, 11.5 and 18.5 m BGL) and the upslope zone of *Sandstone S* (14.5 and 28.5 m BGL). Fe^{2+} was significantly greater ($p < 0.001$) in the sandstone catchment (mean: 639.5 μg/L) compared to the slate site. Analogous to the distribution of Mn^{2+} spatial variability was high with CV values of 157% and 87% in *Sandstone N* and *Sandstone S* respectively. Sampled intervals with highest Fe^{2+} concentrations (>1000 μg/L) followed the distribution of DO, Eh and Mn^{2+} (Table 3).

In the slate catchment, groundwater Mn^{2+} and Fe^{2+} concentrations were typically low (Table 4). Mn^{2+} ranged from 2.3 to 13.3 μg/L, with a mean value of 5.3 μg/L and a CV of 57%. Fe^{2+} ranged from 0.98 to 16.58 μg/L, with a mean groundwater concentration of 7.2 μg/L. Spatial variation was similar between *Slate N* and *Slate S* with CV values of 65% and 62% respectively.

3.3. Excess N_2 concentrations

Excess N_2 in the sandstone catchment was significantly higher than the slate catchment ($p < 0.05$). Mean groundwater concentrations of 1.62 and 0.74 mg N/L were measured in the sandstone and slate catchments respectively. In the sandstone catchment, significant relationships were shown between excess N_2 and hillslopes i.e. *Sandstone N* vs. *Sandstone S* ($p < 0.001$), hillslope zones ($p < 0.05$) and sampling depths ($p < 0.05$). Significant interactions were identified between hillslope and depth ($p < 0.05$) and hillslope zone and depth ($p < 0.05$).

Table 5
Correlation coefficient and significance matrix between NO_3^-, the drivers of denitrification, denitrification rate and reaction products, stable isotope signatures and N_2O emissions for the sandstone and slate catchments.

		Aerobicity		Bacterial energy sources			Denitrification rate & products			N_2O emissions	Stable isotopes		
	NO_3^-	DO	Eh	DOC	Fe^{2+}	Mn^{2+}	RP	Excess N_2	N_2O	N_2O–$EF_{5g}1$	$\delta\,^{15}N_{NO3}$	$\delta\,^{18}O_{NO3}$	$\delta\,^{15}N_{N2O}$
Sandstone catchment													
NO_3^-													
DO	0.78**												
Eh	0.56*	0.72**											
DOC	0.05ns	0.39*	0.19ns										
Fe^{2+}	−0.83**	−0.72**	−0.43*	−0.13ns									
Mn^{2+}	−0.90**	−0.87**	−0.56*	−0.15ns	0.93**								
RP*	−0.94**	−0.87**	−0.64**	−0.16ns	0.90**	0.95**							
excess N_2	−0.77**	−0.79**	−0.54*	0.09ns	0.76**	0.84**	0.85**						
N_2O	0.83**	0.77**	0.72**	0.35ns	−0.71**	−0.79**	−0.87**	−0.52*					
N_2O - $EF_{5g}1$	0.54*	0.58**	0.79**	0.30ns	−0.40ns	−0.52**	−0.60**	−0.28ns	0.85**				
$^{15}N_{NO3}$	−0.51	−0.47*	−0.22ns	−0.15ns	0.42ms*	0.44ms*	0.57*	0.49*	−0.44ms*	−0.21ns			
$^{18}O_{NO3}$	−0.47*	−0.50*	−0.41ms*	−0.07ns	0.38ns	0.45ms*	0.58**	0.57*	−0.44ms*	−0.30ns	0.95**		
$^{15}N_{N2O}$	−0.78**	−0.68**	−0.59**	0.14ns	0.80**	0.86**	0.86**	0.79**	−0.71**	−0.55*	0.37ns	0.46*	
Slate catchment													
NO_3^-													
DO	−0.03ns												
Eh	−0.09ns	0.69**											
DOC	0.19ns	0.00ns	0.01ns										
Fe^{2+}	−0.41ns	−0.05ns	0.22ns	−0.16ns									
Mn^{2+}	−0.05ns	−0.43ns	−0.75**	−0.23ns	−0.07ns								
RP*	−0.08ns	−0.45ns	−0.33ns	−0.15ns	−0.22ns	0.40ns							
excess N_2	0.14ns	−0.48ns	−0.35ns	−0.21ns	−0.27ns	0.36ns	0.96*						
N_2O	−0.12ns	−0.41ns	−0.04ns	0.27ns	0.39ns	−0.27ns	−0.15ns	−0.15ns					
N_2O - $EF_{5g}1$	−0.42ns	−0.37ns	−0.03ns	0.23ns	0.50ns	−0.24ns	−0.12ns	−0.18ns	0.93**				
$^{15}N_{NO3}$	−0.20ns	−0.77**	−0.66*	0.00ns	0.00ns	0.52ns	0.22ns	0.20	0.80**	0.74**			
$^{18}O_{NO3}$	−0.09ns	−0.67*	−0.52ms*	−0.10ns	0.05ns	0.35ns	0.05ns	0.08ns	0.87**	0.72**	0.94**		
$^{15}N_{N2O}$	−0.23ns	0.58ms*	0.44ns	−0.45ns	0.41ns	0.06ns	−0.52ns	−0.54ns	−0.29ns	−0.21ns	−0.35ns	−0.19ns	

** Correlation is significant at the 0.01 level.
* Correlation is significant at the 0.05 level.
ms* Correlation is marginally significant at the 0.1 level.
ns Correlation is not significant.

Sampling depth was positively correlated with excess N_2. Analogous to the zonal relationship described with NO_3^-, a combination of near stream zone and sampling depth had the greatest effect on groundwater excess N_2 (Fig. 3c). Highest excess N_2 corresponded to lowest NO_3- (Fig. 3a) and DO (Fig. 3b). In *Sandstone N*, near stream excess N_2 concentrations were higher than midslope ($p < 0.0001$) and upslope ($p < 0.05$) (Fig. 3c) with lowest values in the midslope zone. In *Sandstone S*, near stream ($p < 0.05$) and upslope ($p < 0.05$) excess N_2 concentrations were higher than midslope values. In stream excess N_2 was lower than groundwater with mean concentrations of 0.1 and 0.2 mg N/L in *Sandstone N* and *Sandstone S*.

Within the slate catchment, no statistically significantly significant differences were identified between excess N_2 and hillslopes, hillslope zones or sample depths. Spatial variation was relatively low (CV: 34%) in both hillslopes, with the exception of the midslope zone of *Slate N* (38 m BGL) were a mean excess N_2 concentration of 3.8 mg N/L was identified. In stream excess N_2 concentrations were similar to groundwater with mean values of 0.12 and 0.22 mg N/L in *Slate N* and *Slate S*.

3.4. N_2O and N_2O emission factors

Groundwater N_2O was significantly higher ($p < 0.0001$) in the sandstone catchment compared to the slate catchment (mean sandstone: 13.0 vs. mean slate: 4.0 μg N/L). In the sandstone catchment, significant relationships were identified between N_2O and hillslopes ($p < 0.01$) with greatest concentrations in *Sandstone N* (Table 3). In *Sandstone N*, near stream N_2O was lower than midslope ($p < 0.05$) and upslope concentrations ($p < 0.05$) with highest values in the upslope zone. In *Sandstone S*, near stream N_2O was lower than midslope ($p < 0.005$), which had the highest N_2O concentrations. No significant difference was shown between the near stream and upslope zones ($p = 0.61$). Depth had contrasting effects on N_2O in both hillslopes which were contingent upon hillslope position. In the near stream zones, depth exhibited a typically negative correlation, however in the midslope and upslope zones the relationship was typically positive (Fig. 3d; Table 3).

In the slate catchment, no significant relationships were identified between N_2O and hillslope ($p = 0.64$), hillslope zones ($p = 0.96$) or sample depths ($p = 0.67$). Spatial variability in both hillslopes was relatively high (mean CV: 72%). This CV was however influenced by four comparative outliers in the dataset namely the near stream zone of *Slate N* (2.5, 11.5 and 42 m BGL) and the midslope zone of *Slate S* (9 m BGL). In both catchments, in-stream N_2O concentrations were lower than groundwater. Mean stream N_2O in the sandstone catchment exceeded the slate catchment by factor of five.

Fig. 5 illustrates the spatial distribution of groundwater and stream water N_2O emission factors ($EF_{5g}1$ and $EF_{5g}2$). $EF_{5g}1$ in the sandstone catchment was significantly higher than the slate catchment ($p < 0.0001$) with the sandstone mean (0.0018) exceeding the slate mean (0.00043) by a factor of three. Mean emission factors for both sandstone hillslopes were comparable (*Sandstone N*: 0.0017 vs. *Sandstone S:* 0.0019) with similar spatial variation (62% vs. 67%). In the sandstone catchment, a significant relationship was found between $EF_{5g}1$ and hillslope zone ($p < 0.001$). In both hillslopes, near stream zones had lower emission factors than midslope and upslope zones ($p < 0.05$). While a statistically significantly relationship with depth was not identified, an analysis of the data, revealed a depth wise relationship analogous to N_2O. In *Sandstone N*, lowest N_2O emission factors were observed at greatest sampling depths (18 and 25 m BGL) in the near stream zone (0.001 and 0.0002). Conversely, highest emission factors were measured at greatest sampling depth (16 and 23.5 m BGL) in the upslope zone (0.0035 and 0.0045) (Fig. 4). In *Sandstone S*, lowest $EF_{5g}1$ corresponded to near stream groundwater, whereas highest values were calculated in the midslope zone.

In the slate catchment, the distribution of $EF_{5g}1$ mirrored the relative abundance of N_2O, with highest emission factors in the near stream zone of *Slate N* (2.5, 11.5 and 42 m BGL) and the midslope zone of *Slate S* (9 m BGL). Spatial variability amongst the remaining groundwater sampling locations was low (CV: 24%). Calculated $EF_{5g}2$ emission factors

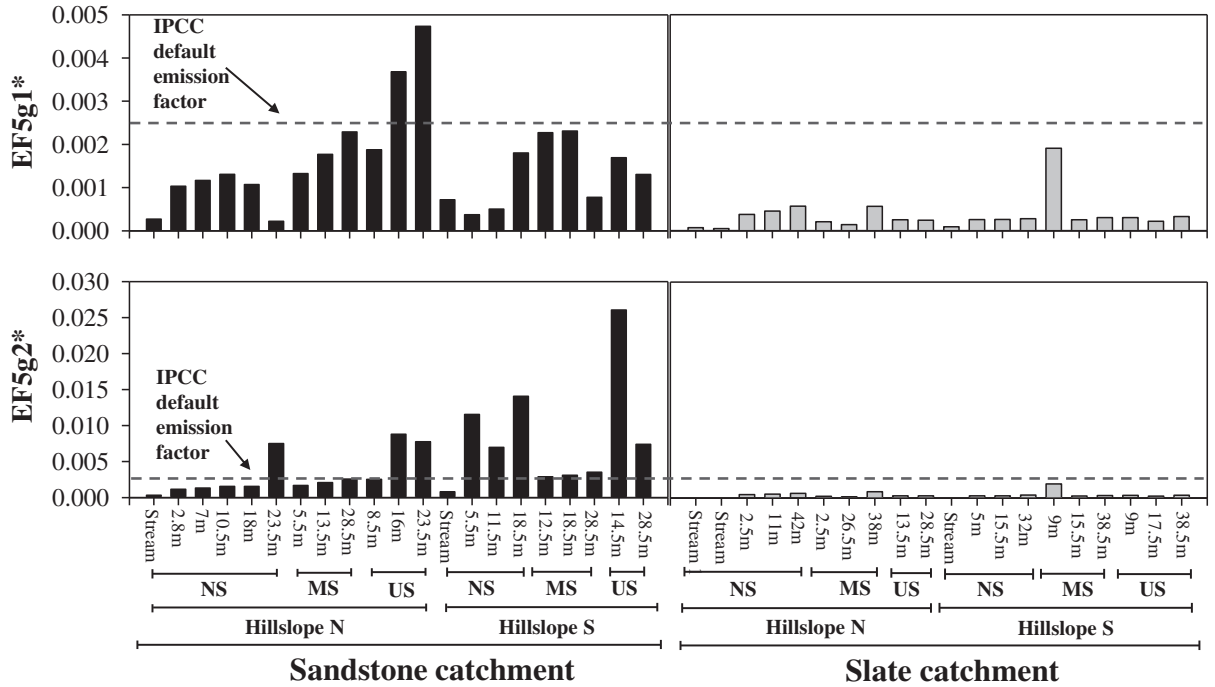

$EF_{5g}1$*: IPCC N_2O emission factor: N_2O/N_{INI} (NO_3^- + NH_4^+ + NO_2^- + organic N + excess N_2 + N_2O)

$EF_{5g}2$*: IPCC N_2O emission factor: N_2O/NO_3^-

Fig. 5. Distribution of N_2O emission factors, mean $EF_{5g}1$ and $EF_{5g}1$ (2013–15), in the sandstone and slate catchments organised by hillslope, slope position and sampling depth.

exceeded corresponding $EF_{5g}1$ values by a factor of 1.3, 1.1, 1.8 and 4.4 in *Slate N*, *Slate S*, *Sandstone N* and *Sandstone S* respectively. $EF_{5g}2$ values were significantly higher ($p < 0.0001$) in the sandstone catchment vs. the slate catchment. $EF_{5g}2$ emission factors were significantly greater than corresponding $EF_{5g}1$values in the near stream zones of both *Sandstone N* and *Sandstone S*, with lowest values in the midslope zones. Conversely the spatial distribution of $EF_{5g}2$ in the slate catchment was similar to the distribution of $EF_{5g}1$.

3.5. Denitrification reaction progress (RP)

Denitrification reaction progress (RP) is shown Tables 3 and 4 for the sandstone and slate catchments respectively. Groundwater RP in the sandstone catchment was significantly higher ($p < 0.005$) than the slate catchment ranging from 0.04–0.94. In the sandstone catchment significant interactions were identified between hillslope and hillslope zone ($p < 0.05$) and hillslopes zone and depth ($p < 0.05$). A combination of near stream zone and increasing depth had the greatest effect on RP values ($p < 0.05$). In *Sandstone N*, RP values in the near stream zone were significantly higher ($p < 0.05$) than up gradient values. There was a significant positive correlation between RP and sampling depth. In *Sandstone S*, the near stream and upslope zones had greater RP than the midslope zone ($p < 0.001$; $p < 0.05$) with no significant difference between near stream and upslope ($p = 0.91$). RP values were elevated at all sample depths in the near stream zone (Table 3).

In the slate catchment, RP ranged from 0.02 to 0.34, with a mean value of 0.11 (Table 4). No significant relationships were identified between RP and hillslope, hillslope zone or sampling depth.

3.6. Denitrification vs. dilution

To differentiate between denitrification and dilution, the distribution Cl^- (conservative) versus NO_3^- (non-conservative) was examined. In the sandstone catchment, the mean Cl^- concentration was 31.38 mg/L. Spatial variation across hillslope zones and sampling depths was low, with CV values of 6% and 3% in *Sandstone N* and *Sandstone S*, respectively. Conversely, the ratio of NO_3^- to Cl^- showed considerable spatial variation (CV *Sandstone N*: 38%; CV *Sandstone S*: 110%).

In the slate catchment, the spatial mean Cl^- concentration was 19.27 mg/L, approximately 40% lower than the sandstone catchment (Table 4). Spatial variation across both hillslopes was low (mean CV: 16.6%). In contrast to the sandstone catchment, the ratio of NO_3^- to Cl^- was relatively uniform in both hillslopes with a range of 0.35 to 0.55 and a CV of 14%.

3.7. Factors affecting denitrification

3.7.1. Dissolved oxygen

The relationships between groundwater DO and RP, NO_3^-, excess N_2 and N_2O for both study catchments are presented in Fig. 6. A breakdown of catchment specific relationships are presented as a correlation matrix in Table 5. In the sandstone catchment, strongly negative correlations were identified between groundwater DO and RP ($r = -0.87$, $p < 0.0001$). DO was negatively correlated with excess N_2 ($r = -0.79$, $p < 0.0001$) and positively correlated with NO_3^- ($r = 0.78$, $p < 0.001$) (Fig. 6). The relationship between N_2O and DO in the sandstone catchment, while statistically positive ($r = 0.77$, $p < 0.05$) was complex. Highest N_2O occurred at DO between 4 and 8 mg/L with significantly lower concentrations between 0 and 3 mg/L and 8 to 10 mg/L (Fig. 6). In contrast to the sandstone catchment, groundwater in the slate catchment was consistently aerobic, with no significant correlations identified between DO and RP, NO_3^-, excess N_2 or N_2O.

3.7.2. Bacterial energy sources

In the sandstone catchment, concentrations of reduced metals (Mn^{2+} and Fe^{2+}) were highly dependent on aquifer aerobicity

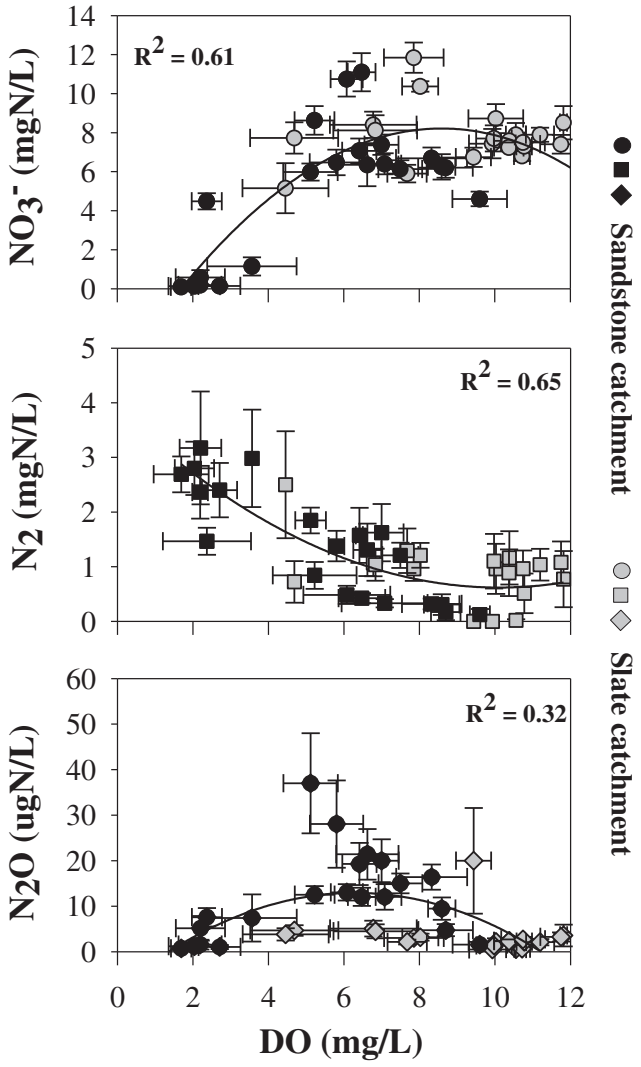

Fig. 6. Groundwater dissolved oxygen (DO) plotted against NO_3^-, excess N_2 and N_2O for the sandstone (black symbols) and slate (grey symbols) catchments.

(Table 5). Mn^{2+} was negatively correlated with DO ($r = -0.87$; $p < 0.0001$) and Eh ($r = -0.56$; $p < 0.001$). Similarly, Fe^{2+} was negatively correlated with DO ($r = -0.72$; $p < 0.0001$) and Eh ($r = -0.43$; $p < 0.05$), and positively correlated with Mn^{2+} ($r = 0.93$; $p < 0.0001$) (Table 5). Significant positive relationships were discovered between Mn^{2+} and RP ($r = 0.95$, $p < 0.0001$) and Fe^{2+} and RP ($r = 0.90$, $p < 0.0001$). Strongly negative relationships were shown between Fe^{2+} and NO_3^- ($r = -0.83$, $p < 0.005$) and between Mn^{2+} and NO_3^- ($r = -0.90$, $p < 0.0001$). N_2O was negatively correlated with Fe^{2+} ($r = -0.71$, $p < 0.005$) and Mn^{2+} ($r = -0.79$, $p < 0.005$). Conversely, excess N_2 was positively correlated with Fe^{2+} ($r = -0.76$, $p < 0.0001$) and Mn^{2+} ($r = 0.84$, $p < 0.0001$). No significant relationships were observed between DOC and excess N_2 or N_2O. DOC did however exhibit a weakly negative correlation with DO ($r = -0.39$, $p = 0.087$). In the slate catchment, no significant relationships were identified between reduced bacterial energy sources (DOC, Mn^{2+} & Fe^{2+}) and RP, DO, NO_3^-, N_2O or excess N_2.

3.7.3. Denitrification reaction progress (RP)

DO concentrations and the abundance of reduced metals (Mn^{2+} and Fe^{2+}) were the dominant factors affecting denitrification RP. The spatial relationships between groundwater RP and NO_3^-, excess N_2 and N_2O for both study catchments are presented in Fig. 7 and Table 5. In the sandstone catchment, RP exhibited a strongly negative correlation with NO_3^-

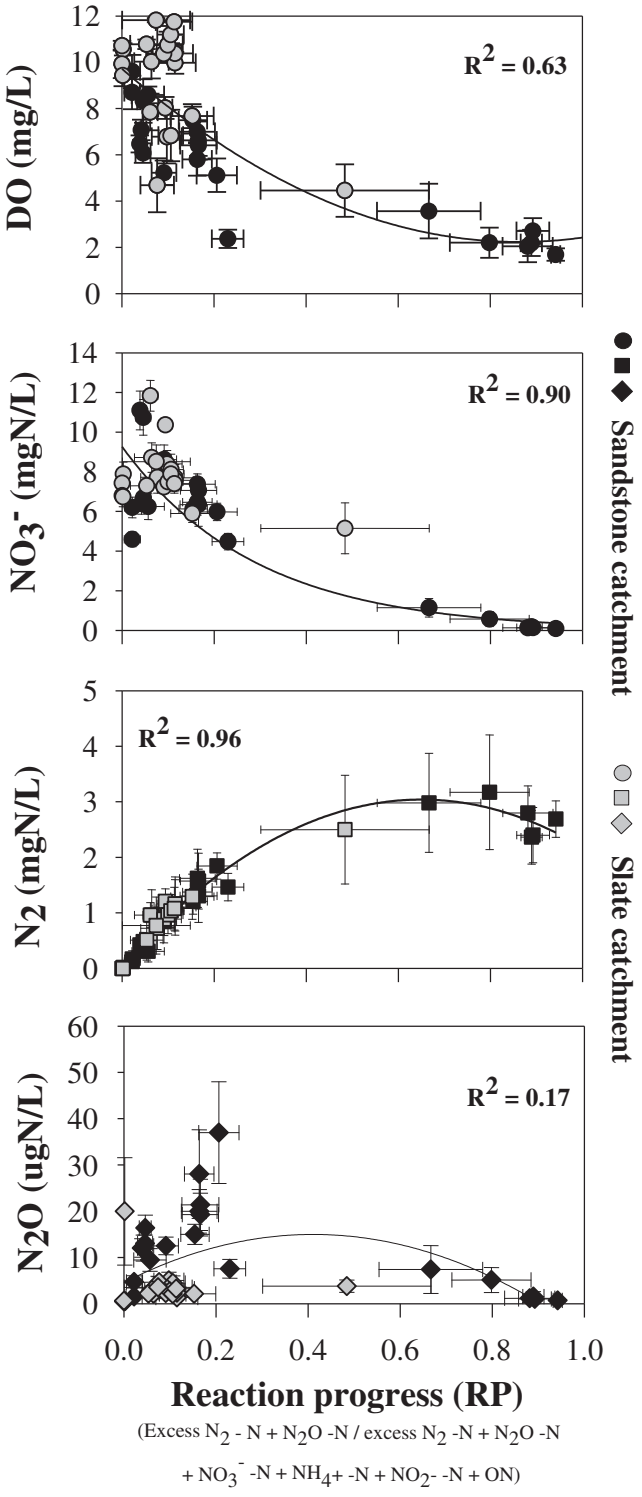

Fig. 7. Groundwater reaction progress (RP) plotted against dissolved oxygen (DO), NO_3^-, excess N_2 and N_2O for the sandstone (black symbols) and slate (grey symbols) catchments.

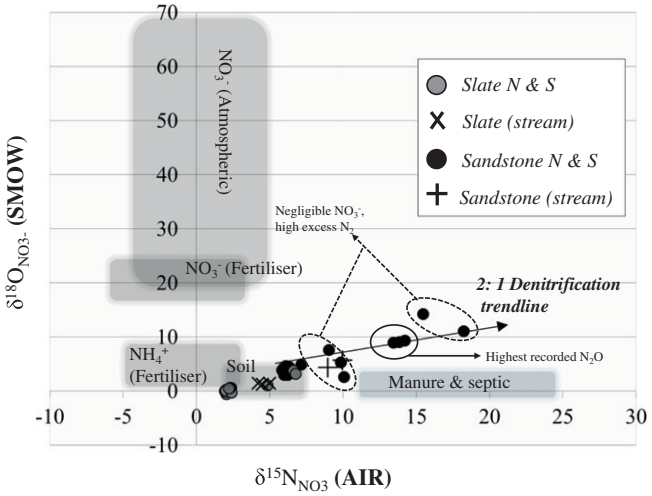

Fig. 8. $\delta^{18}O$ versus $\delta^{15}N$ values of NO_3^- for groundwater samples collected in September 2014 Also shown are the $\delta^{18}O$ and $\delta^{15}N$ ranges typical of NO_3^- sources and a 2:1 trendline of $\delta^{18}O$ versus $\delta^{15}N$ which is typical of denitrification progress (after Kendall et al., 2007).

($r = -0.94$, $p < 0.0001$) and N_2O ($r = -0.87$, $p < 0.0001$). Conversely, there was a significantly positive relationship between RP and excess N_2 ($r = 0.85$, $p < 0.0001$). Lowest NO_3^- concentrations corresponded to RP >0.60, which was consistent with the highest measured excess N_2. N_2O concentrations were low at RP <0.10 and >0.60, with highest concentrations occurring between 0.10 and 0.3 (Fig. 7). In slate catchment, no significant correlations were identified between RP and NO_3^- or N_2O

3.8. Stable isotope values

$\delta^{15}N_{NO3}$ and $\delta^{18}O_{NO3}$ were significantly higher in the sandstone catchment compared to the slate site (Fig. 8) ($p < 0.0001$). In the sandstone catchment, $\delta^{15}N_{NO3}$ ranged from +6.0 to 18.2‰ with a mean ratio of 9.6‰. $\delta^{18}O_{NO3}$ ranged from 3.0 to 11.6‰, with a mean value of 6.3‰. Highest values of both $\delta^{15}N_{NO3}$ and $\delta^{18}O_{NO3}$ occurred in the near stream zones of *Sandstone N* and *Sandstone S* and in the upslope zones of both hillslopes. $\delta^{15}N_{NO3}$ was negatively correlated with NO_3^- ($r = -0.51$, $p < 0.05$) (Fig. 9), DO ($r = -0.47$, $p < 0.05$) and N_2O ($r = -0.44$, $p < 0.1$) and positively related to RP ($r = 0.58$, $p < 0.01$) and excess N_2 ($r = 0.49$, $p < 0.05$) (Table 5). $\delta^{15}N_{N2O}$ was significantly higher in the sandstone catchment versus than the slate catchment ($p < 0.05$). In the sandstone catchment, $\delta^{15}N_{N2O}$ ranged from −13.6 to 9.7‰, with a mean value of 4.9‰ and exhibited both positive and negative enrichment ratios (Fig. 9). $\delta^{15}N_{N2O}$ was negatively correlated with NO_3^- ($r = -0.78$, $p < 0.01$) (Fig. 8), DO ($r = -0.68$, $p < 0.01$) and N_2O ($r = -0.71$, $p < 0.01$) (Table 5). Conversely $\delta^{15}N_{N2O}$ was positively correlated with RP ($r = 0.86$, $p < 0.05$) and excess N_2 ($r = 0.79$, $p < 0.05$).

In the slate catchment, $\delta^{15}N_{NO3}$ ranged from +1.9 to 6.8‰ with a mean value of 3.3‰. $\delta^{18}O_{NO3}$ ranged from −0.5 to +3.8‰ with a mean enrichment ratio of 0.8‰. $\delta^{15}N_{NO3}$ was not correlated with NO_3^-, RP or excess N_2 but did exhibit significant relationships with DO ($r = -0.77$, $p < 0.05$) and N_2O ($r = 0.8$, $p < 0.05$). $\delta^{15}N_{N2O}$ was consistently negative, ranging from −20.8 to −4.6‰ (mean: −3.2‰) (Fig. 9). No significant correlations were identified between $\delta^{15}N_{N2O}$ and NO_3^-, RP, excess N_2 or N_2O. A marginally significant correlation was shown between $\delta^{15}N_{N2O}$ and DO ($r = 0.58$, $p < 0.1$).

4. Discussion

The study highlighted a complex mosaic of NO_3^- removal capacity between study catchments, between catchment hillslopes, and within catchment hillslopes. A range of spatially variable, physical and hydrogeochemical parameters where identified to regulate 1) NO_3^- removal capacity, 2) gaseous accumulation and 3) indirect N_2O emissions. Previous research has documented that low permeability aquifers coupled with the presence of denitrifying bacteria, reducing conditions and the availability of bacterial energy sources create zones of enhanced denitrification potential (Brettar et al., 2002; Jahangir et al., 2012a; Rissmann,

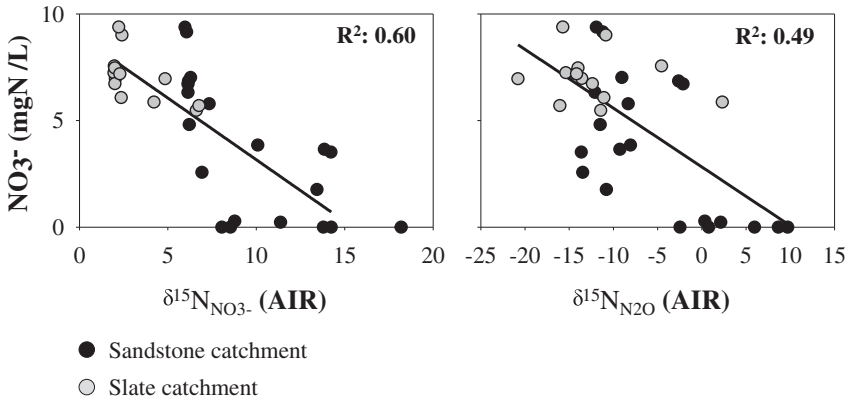

Fig. 9. $\delta^{15}N_{NO3}$ $\delta^{15}N_{N2O}$ values vs. NO_3^- in the sandstone and slate catchments.

2011; Thayalakumaran et al., 2008. While a number of these criteria may be met within a given catchment, the absence of one can arrest the denitrification process and resultant NO_3^- attenuation. The combined analysis of physical and hydrogeochemical factors and stable isotope signatures versus the natural abundance of NO_3^-, excess N_2 and N_2O revealed a tale of two catchments. The slate catchment was characterised by hydrogeochemical uniformity with limited groundwater NO_3^- reduction. The sandstone catchment exhibited spatially heterogeneous zones of incomplete and complete NO_3^- removal. Despite significantly higher applications of organic and inorganic N in the sandstone catchment, mean groundwater and stream NO_3^- concentrations were significantly lower. The positive mitigation effect of NO_3^- removal in the sandstone catchment was however concomitant with substantially greater emissions of N_2O.

4.1. Denitrification vs dilution

The ratio between NO_3^- and Cl^- was used as an indirect indictor to differentiate between denitrification and dilution processes, with Cl^- acting conservatively and NO_3^- acting non-conservatively along a flow path. In the sandstone catchment, low concentrations of NO_3^- with unaffected Cl^- resulted in low NO_3^-/Cl^- ratios in various zones throughout each hillslope (Table 4). Similar to Fenton et al. (2009), this suggests that groundwater denitrification was the dominant factor regulating groundwater NO_3^- occurrence. In the slate catchment high hillslope NO_3^-/Cl^- ratios and a proportional decrease of NO_3^- and Cl^- progressing downslope, suggest dilution as the dominant NO_3^- attenuating mechanism.

Stable isotope signatures were used to identify transformational processes in the study catchments. The bacteria involved in denitrification preferentially metabolise the lighter NO_3^- isotopes. As such, an enrichment of the heavier NO_3^- isotopes in groundwater provides direct evidence of denitrification. In the sandstone catchment, contemporaneous isotopic enrichment of $\delta^{15}N_{NO3}$ and $\delta^{18}O_{NO3}$, along an approximate 2:1 regression trend line signified denitrification (Fig. 8). Previous authors reported a comparable trend in the relative proportion of $\delta^{15}N_{NO3}$ vs. $\delta^{18}O_{NO3}$ as representative of denitrification with ratios of 1.5:1 identified in Baily et al. (2011) and 2:1 in Aravena and Robertson (1998), Mengis et al. (1999) and Panno et al. (2006). Correlations between $^{15}N_{NO3}$ and NO_3^- and $\delta^{15}N_{N2O}$ and NO_3^- indicated both reduction of NO_3^- and production of N_2O in groundwater (Fig. 9). In highly denitrifying zones, N_2O was further reduced to excess N_2, as indicated by positive $\delta^{15}N_{N2O}$ values e.g. Well et al. (2012). N_2O reduction was coincident with high RP, low NO_3^- and high excess N_2. In the slate catchment a lack of correlation between $\delta^{15}N_{NO3}$, $\delta^{15}N_{N2O}$ and NO_3^- (Table 5) indicated that denitrification was unlikely. Uniformity in groundwater NO_3^- concentrations was coincident with low RP. Moreover, $\delta^{15}N_{NO3}$ and $\delta^{18}O_{NO3}$ ratios (Fig. 5) were reflective of source rather than transformational signatures supporting the contention that dilution rather than denitrification dominated in the slate catchment.

4.2. Catchment N dynamics & denitrification capacity

In spite of a 79% greater surface application of available N to the sandstone hillslopes (Table 2), mean stream NO_3^- concentrations were 32% lower than the slate sites (Fig. 2). This is part due to the presence of long term grassland cover in the sandstone catchment versus tillage in the slate catchment. Tillage catchments undergo periodic ploughing and reseeding with associated bare soils resulting in higher N leaching losses from soil to groundwater and lower DOC loss which limits subsurface denitrification (Jahangir et al., 2014). The greater propensity for N in loss in arable catchments was reflected in a mean FracLEACH value of 42.5% in the slate catchment versus 17.5% in the grassland catchment (Table 2). While FracLEACH was considerably higher at the slate hillslopes, the associated N loads reaching the water table were comparable with 55 and 60 kg N/ha/yr. reaching the water table in the sandstone and slate catchments respectively. These are similar to leaching losses reported by Huebsch et al. (2013) in intensively managed grassland and Premrov et al. (2012) in spring barley. Comparing shallow groundwater NO_3^- with stream NO_3^- concentrations in both catchments revealed a 43% reduction in NO_3^- from groundwater to stream in the sandstone catchment versus a 7% reduction in the slate site. It is likely therefore that a combination of agricultural practises and hydrogeochemical transformations acted to mitigate stream N enrichment in the denitrifying sandstone catchment.

Analogous to the findings of Hinkle et al. (2007), Weymann et al. (2008) and Jahangir et al. (2012a) the sandstone catchment was characterised by highest NO_3^- in shallow groundwater, typically decreasing with depth (Fig. 2). Aligned to Fenton et al. (2009), highest NO_3^- concentrations were observed in high permeability quaternary deposits. Underlying the Quaternary deposits in both sandstone hillslopes, a layered distribution of bedrock permeability (Ksat) was evident, becoming less permeable with depth (Table 2). In the sandstone catchment, weathered bedrock zones with high Ksat allowed a fast migration of NO_3^- contaminated groundwater with limited scope for microbial attenuation. Lower Ksat with depth resulted in a longer residence time of both groundwater NO_3^- and DO. With a longer residence time in the sandstone catchment, denitrification was promoted, resulting in lower NO_3^- concentrations. This contention was supported by significant negative correlations between Ksat and NO_3^- and Ksat and DO (Fig. 4). High permeability weathered zones ranging in thickness from 4 to 11 m and 5 to 18 m in *Slate N* and *Slate S* respectively (Table 1), aligned with a lack of correlation between Ksat and NO_3^- or DO suggested that rapid groundwater flow restricted denitrification progress.

Groundwater DO concentration was the dominant control on RP, NO_3^-, excess N_2 and N_2O. Analogous to field studies undertaken in highly denitrifying aquifers (Blicher-Mathiesen et al., 1998; Well et al., 2012), significant correlations were identified between DO, NO_3^-, N_2O and excess N_2. Previous studies have documented a DO range between <1 and 4 mg/L as supportive of denitrification (Rivett et al., 2008). In the sandstone catchment, negligible groundwater NO_3^- concentrations corresponded to DO <3.5 mg/L and Eh <30 mV. In low oxygen environments, denitrification results in the sequential reduction of NO_3^- to N_2O to excess N_2. Near stream zones exhibited a significant capacity for complete denitrification to excess N_2, where low DO and high RP corresponded to negligible NO_3^-, low N_2O and high excess N_2. The correlation between the relative depth of the water table and DO (Fig. 4), indicated that a water table close to the ground surface promoted lower groundwater DO and NO_3^- concentrations. In near stream zones where water tables are typically <1 m BGL, the development of anaerobic conditions, and as a result denitrifying environments are promoted. With the exception of the upslope zone of *Sandstone S* which was a relative outlier, the range of DO (5.1–8.6 mg/L) in the midslope and upslope zones of the sandstone catchment inhibited complete denitrification to excess N_2, instead arresting the denitrification reaction at the N_2O production stage. Maximum water table depths in the midslope and upslope zones of the sandstone hillslopes ranged from 4 to 14 m BGL. Higher DO in the midslope and upslope hillslope zones of the sandstone catchment support the results of Young et al. (2013), where substantially greater diffusive and advective transport of DO into groundwater underling unsaturated zones in excess of 5 m thickness was observed. Similarly, Fenton et al. (2009) and Jahangir et al. (2012a, 2013) described highest NO_3^- and N_2O in groundwater underlain by thick unsaturated zones. Results of the statistical model and correlation analysis suggest therefore that near stream zones promote complete reduction of NO_3^- to excess N_2 whereas in midslope and upslope zones, N_2O is the dominant denitrification reaction product.

Whereas the sandstone catchment exhibited a complex interplay between groundwater DO, RP, NO_3^-, N_2O and excess N_2, the slate catchment was characterised by a lack of significant correlation. In the slate catchment, aerobic conditions at all hillslope zones and depths restricted the development of denitrifying hotspots, with correspondingly low RP values throughout (Fig. 7). This resulted in uniformly high NO_3^-, low excess N_2 and low N_2O. Although permeability was typically high, low Ksat zones in *Slate N* did not promote complete denitrification. Moreover intermediate DO concentrations which were comparable to the sandstone catchment resulted in significantly lower N_2O production.

Reduction of both DO and NO_3^- requires a bacterial energy source. Under low DO concentrations, NO_3^- is the most energetically favourable electron acceptor for bacterial metabolism. Energy sources include surface derived DOC and/or solid phase carbon, Fe^{2+}, Mn^{2+} and S^- (Rivett et al., 2008) dissolved under anaerobic conditions. Mean DOC of 2.5 and 1.8 mg/L in the sandstone and slate catchments respectively was aligned with the low concentrations described in previous studies (<5 mg/L) (Rivett et al., 2008). A lack of bioavailable DOC is a dominant limiting factor on groundwater denitrification rates (Starr and Gillham, 1993; Wassenaar, 1995). In both catchments there was a lack of correlation between DOC and RP, NO_3^-, excess N_2 or N_2O (Table 5). The required stoichiometry of 1:1.25 between NO_3^- and DOC (Dimkić et al., 2008; Thayalakumaran et al., 2008) indicated that the levels of DOC in the saturated zones of both catchments could not support heterotrophic denitrification.

Typical of grassland agriculture, inputs of organic N to the sandstone hillslopes were high (Table 2). Previous research (Pabich et al., 2001) documented an exponential decrease of DOC with depth below the water table. Conversely, in the sandstone catchment, spatial variability in DOC was uniformly low in both shallow and deeper groundwater pathways. During transport through the unsaturated zone DOC is biodegraded via oxidation to CO_2^-, which in turn reduces DO. Mean DO of 5.0 mg/L in shallow groundwater (<10 m BGL) of the sandstone catchment, aligned with low spatial variation of DOC, suggested DOC consumption and DO reduction prior to reaching the water table. A significantly negative correlation between DOC and DO (Table 5) within the saturated zone suggested that a proportion of the leached DOC was bioavailable (Chapelle et al., 2012). Organic N input to the sandstone hillslopes was on average 116% greater than the slate sites. Conversely, mean shallow groundwater (<10 m BGL) DOC concentrations were only 15% greater. DOC consumption prior to reaching the water table in the sandstone catchment was therefore a likely factor. Lower lability soil organic carbon is typical of long term arable cropping systems compared to grassland dominated catchments (Premrov et al., 2012). Organic inputs were not sufficient to support DO reduction in the slate catchment, as indicated by low DOC and high DO in both hillslopes.

When labile DOC is not sufficient in supply or has been biodegraded during DO reduction, solid phase electron donors must be present to support denitrification. When anaerobicity prevails, electron donors such as Mn^{2+} and Fe^{2+} can accumulate along a flow path (Tesoriero and Puckett, 2011). Several studies have hypothesised autotrophic denitrification in DOC limited aquifers (Green et al., 2008; Heffernan et al., 2012; Weymann et al., 2008). In the sandstone catchment, strongly positive correlations were identified between Fe^{2+}/Mn^{2+}, RP and excess N_2 (Table 5). While RP and excess N_2 increased with increasing Fe^{2+} and Mn^{2+}; NO_3^-, N_2O, DO and Eh decreased signifying autotrophic denitrification. If an aquifer lacks solid phase electron donors (Liao et al., 2012), DOC concentrations in recharge are too low to support DO reduction (Thayalakumaran et al., 2015) or residence times are too short to support significant solid phase dissolution (Vidon and Hill, 2005), denitrification is suppressed. It is likely that this was the case in the slate catchment.

4.3. Catchment N_2O concentrations & emissions

The spatial mean groundwater N_2O concentrations (sandstone: 13 μg N/L; slate: 4 μg N/L) observed in the present study were comparable those observed by other authors. Vilain et al. (2012) measured mean concentrations of 37.4, 11.1 and 9.5 μg N/L in the upslope, midslope and near stream zones of a limestone aquifer, while Mühlherr and Hiscock (1998) described mean N_2O concentrations 33, 12.5 and 4.3 μg N/L in three limestone aquifers. A commonality throughout the literature indicates that N_2O accumulation is spatially variable with CVs of 217% (Yanai et al., 2003), 258% (von der Heide et al., 2009) compared with 72–99% in slate and sandstone catchment. At the average sampling temperature (11 °C), the expected air equilibrium concentration of N_2O in groundwater is 0.33 μg N/L (Mühlherr and Hiscock, 1998). Mean groundwater N_2O was 39 and 12 times greater than atmospheric equilibrium in the sandstone and slate catchments respectively. Furthermore, the maximum recorded N_2O concentration in the sandstone catchment exceeded atmospheric equilibrium by a factor of 300. Any N_2O in excess of atmospheric equilibrium will degas to the atmosphere once groundwater rises to the surface, enters the stream or diffuses through the unsaturated zone. The described concentrations in both catchments therefore represent potential greenhouse gas sources to the atmosphere. Directly measured N_2O concentrations however do not represent the actual emissions from the aquifer to the atmosphere (Weymann et al., 2008). N_2O may increase or decrease with greater residence time prior to its eventual release point. Von der Heide et al. (2009) measured negligible fluxes of N_2O vertically from groundwater to the atmosphere in spite of high N_2O concentrations in shallow groundwater. Given that highest N_2O accumulation occurred at depth, it is likely that advective rather than diffusive transport of groundwater N_2O dominated in the present study. In stream N_2O concentrations provide a measurement groundwater derived N_2O degassing to the atmosphere. In the sandstone catchment, mean near stream groundwater N_2O was 95% lower than up gradient concentrations while mean stream N_2O concentrations were 68% lower than near stream groundwater. Analogous to Höll et al. (2005) it is likely that groundwater N_2O was

consumed during passage from groundwater to the stream. While substantially lower than up gradient groundwater concentrations, stream N_2O in *Sandstone N* and *Sandstone S* were 4.5 and 16 times atmospheric equilibrium respectively, indicating a net contribution to atmospheric greenhouse gas emissions. In the slate catchment, mean stream N_2O was 164% less than the sandstone catchment. In the present study, two available methods were used to calculate EF_{5g}, producing contrasting results. $EF_{5g}1$ takes into account all forms of reactive N including the products of denitrification. The results of the $EF_{5g}1$ analysis support the IPCC (2006) downward revision from 0.015 to 0.0025 with mean emission factors of 0.0018 and 0.0004 in the sandstone and slate catchments respectively. Emissions above the IPCC default were consistent with highest N_2O concentrations in the midslope and upslope zones of the sandstone hillslopes (Fig. 5); however as demonstrated, actual N_2O transport to the streams did not reflect the up gradient maxima. The calculation of $EF_{5g}2$ considers NO_3^- and N_2O only. In the sandstone catchment, where there was significant denitrification, $EF_{5g}2$ overestimated emissions, with the mean value of 0.005 exceeding $EF_{5g}1$ by 113%. Highest $EF_{5g}1$ values were consistent with lowest N_2O concentrations (Fig. 5), and reflected low NO_3^- (resulting from conversion to excess N_2) rather than high N_2O. Conversely, in the slate catchment, $EF_{5g}2$ exceeded $EF_{5g}2$ by 15%. As such, $EF_{5g}2$ can only be considered as an accurate measurement in aquifers with limited denitrification.

5. Conclusion

The capacity of hillslope hydrologic systems to naturally mitigate groundwater and stream NO_3^- is site specific. There exists a hierarchy of scale whereby physical factors including agronomy, water table elevation and permeability determine the hydrogeochemical properties of the aquifer. The hydrochemical signature (DO, Eh and bacterial energy source availability) can in turn either support or suppress denitrification and subsequent NO_3^- reduction. DO concentration was the dominant control, explaining 87%, 78% and 77% of the variance in groundwater RP, NO_3^- and N_2O respectively in the denitrifying sandstone catchment. Information on aquifer geochemistry can therefore be used as a predictor of denitrification capacity, NO_3^- and N_2O concentrations in different hydrological settings. In catchments with sufficient organic N inputs, DOC and water table elevation regulate the concentration of DO reaching the water table surface. In the saturated zone, permeability distribution controls the dissolution of solid phase electron donors, which in turn drives further DO reduction and the development of denitrifying conditions. In catchments were organic inputs are not sufficient to promote DO reduction, and residence times are too short to facilitate solid phase electron donor dissolution, denitrification progress is arrested, with correspondingly higher stream and groundwater NO_3^- abundance. An entire aquifer or catchment cannot be characterised as having high or low denitrification potential. In the sandstone catchment, complete removal of NO_3^- was enhanced in near stream denitrifying hot spots. In base flow dominated catchments, all groundwater entering the stream must first pass through these denitrifying zones, which has a positive effect on stream NO_3^- mitigation. Near stream zones should therefore be prioritised and protected, with consideration given to the location of land drainage, which can act to bypass near stream NO_3- removal zones. Highest N_2O abundance occurred in up-gradient zones of the sandstone hillslopes, greatly exceeding atmospheric equilibrium concentrations, while also in excess of the IPCC EF_{5g} threshold. The upslope N_2O maxima were not however manifested in the sandstone streams, highlighting that groundwater discharge through near stream zones was not only paramount to NO_3^- reduction, but also vital to N_2O mitigation. While stream N_2O was substantially lower than groundwater, mean values were significantly greater than atmospheric equilibrium, particularly in the sandstone catchment. The positive environmental effect of NO_3^- reduction was therefore concomitant with a net source of harmful greenhouse gas emissions. A review of the IPCC methodology ($EF_{5g}1$ and $EF_{5g}2$ revealed that $EF_{5g}2$ can only be used effectively in non-denitrifying catchments, while mean $EF_{5g}1$ calculations supported the downward IPCC revision of N_2O emissions from groundwater.

Acknowledgements

The first author gratefully acknowledges funding received from the Teagasc Walsh Fellowship Scheme (2012050). The first author also wishes to acknowledge all of the field and laboratory staff in Teagasc Johnstown Castle, with a special thank you to the members of the Agricultural Catchments Programme team.

Appendix A. Supplementary data

Supplementary data to this article can be found online at http://dx.doi.org/10.1016/j.scitotenv.2016.11.083.

References

Aravena, R., Robertson, W.D., 1998. Use of multiple isotope tracers to evaluate denitrification in ground water: study of nitrate from a large-flux septic system plume. Groundwater 36 (6), 975–982.
Baily, A., Rock, L., Watson, C.J., Fenton, O., 2011. Spatial and temporal variations in groundwater nitrate at an intensive dairy farm in south-east Ireland: insights from stable isotope data. Agric. Ecosyst. Environ. 144 (1), 308–318.
Barrett, M., Jahangir, M.M.R., Lee, C., Smith, C.J., Bhreathnach, N., Collins, G., Richards, K.G., O'Flaherty, V., 2013. Abundance of denitrification genes under different piezometer depths in four Irish agricultural groundwater sites. Environ. Sci. Pollut. Res. 20, 6646–6657.
Blicher-Mathiesen, G., McCarty, G.W., Nielsen, L.P., 1998. Denitrification and degassing in groundwater estimated from dissolved dinitrogen and argon. J. Hydrol. 208 (1), 16–24.
Bouwman, A., 1990. Exchange of greenhouse gases between terrestrial ecosystems and the atmosphere. Soils Greenh. Eff. 61–127.
Bower, H., Rice, R., 1976. A slug test for determining hydraulic conductivity of unconfined aquifers with completely or partially penetrating wells. Water Resour. Res. 12, 423-423.
Brettar, I., Sanchez-Perez, J.-M., Trémolieres, M., 2002. Nitrate elimination by denitrification in hardwood forest soils of the Upper Rhine floodplain–correlation with redox potential and organic matter. Hydrobiologia 469, 11–21.
Butler Jr., J.J., 1997. The Design, Performance, and Analysis of Slug Tests. Crc Press.
Chapelle, F.H., Bradley, P.M., McMahon, P.B., Kaiser, K., Benner, R., 2012. Dissolved oxygen as an indicator of bioavailable dissolved organic carbon in groundwater. Groundwater 50, 230–241.
Clough, T.J., Addy, K., Kellogg, D.Q., Nowicki, B.L., Gold, A.J., Groffman, P.M., 2007. Dynamics of nitrous oxide in groundwater at the aquatic–terrestrial interface. Glob. Chang. Biol. 13, 1528–1537.
De Klein, C.A., Sherlock, R.R., Cameron, K.C., Van Der Weerden, T.J., 2001. Nitrous oxide emissions from agricultural soils in New Zealand — a review of current knowledge and directions for future research. J. R. Soc. N. Z. 31, 543–574.
De Klein, C., Novoa, R.S., Ogle, S., Smith, K., Rochette, P., Wirth, T., Mcconkey, B., Mosier, A., Rypdal, K., Walsh, M., 2006. N_2O Emissions From Managed Soils and CO_2 Emissions From Lime and Urea Application. IPCC Guidelines for National Greenhouse Gas Inventories, Prepared by the National Greenhouse Gas Inventories Programme 4 pp. 1–54.
Dennis, S.J., Cameron, K.C., Di, H.J., Moir, J.L., Staples, V., Sills, P., Richards, K.G., 2012. Reducing nitrate losses from grazed grassland in Ireland using a nitrification inhibitor (DCD). Biol. Environ. 112B, 79–89.
Dimkić, M.A., Brauch, H.-J., Kavanaugh, M., 2008. Groundwater management in large river basins. Water Intell. Online 7 (9781780401843).
Fealy, R., Buckley, C., Mechan, S., Melland, A., Mellander, P., Shortle, G., Wall, D., Jordan, P., 2010. The Irish agricultural catchments programme: catchment selection using spatial multi-criteria decision analysis. Soil Use Manag. 26, 225–236.
Fenton, O., Richards, K.G., Kirwan, L., Khalil, M.I., Healy, M.G., 2009. Factors affecting nitrate distribution in shallow groundwater under a beef farm in South Eastern Ireland. J. Environ. Manag. 90, 3135–3146.
Fenton, O., Schulte, R.P., Jordan, P., Lalor, S.T., Richards, K.G., 2011. Time lag: a methodology for the estimation of vertical and horizontal travel and flushing timescales to nitrate threshold concentrations in Irish aquifers. Environ. Sci. Pol. 14, 419–431.
Geological Society of Ireland, 2016. Groundwater webmapping.Available. https://www.gsi.ie/Programmes/Groundwater/Groundwater+web+mapping.htm (Last accessed 1st June 2016).
Green, C.T., Puckett, L.J., Böhlke, J.K., Bekins, B.A., Phillips, S.P., Kauffman, L.J., Denver, J.M., Johnson, H.M., 2008. Limited occurrence of denitrification in four shallow aquifers in agricultural areas of the United States. J. Environ. Qual. 37, 994–1009.
Gruber, N., Galloway, J.N., 2008. An Earth-system perspective of the global nitrogen cycle. Nature 451, 293–296.
Harty, M.A., Forrestal, P.J., Watson, C.J., McGeough, K.L., Carolan, R., Elliot, C., Krol, D., Laughlin, R.J., Richards, K.G., Lanigan, G.J., 2016. Reducing nitrous oxide emissions by changing N fertiliser use from calcium ammonium nitrate (CAN) to urea based formulations. Sci. Total Environ. 563–564, 576–586.
Heffernan, J., Albertin, A., Fork, M., Katz, B., Cohen, M., 2012. Denitrification and inference of nitrogen sources in the karstic Floridan Aquifer. Biogeosciences 9, 1671–1690.

Hinkle, S.R., Böhlke, J., Duff, J.H., Morgan, D.S., Weick, R.J., 2007. Aquifer-scale controls on the distribution of nitrate and ammonium in ground water near La Pine, Oregon, USA. J. Hydrol. 333, 486–503.
Hiscock, K., Bateman, A., Mühlherr, I., Fukada, T., Dennis, P., 2003. Indirect emissions of nitrous oxide from regional aquifers in the United Kingdom. Environ. Sci. Technol. 37, 3507–3512.
Höll, B.S., Jungkunst, H.F., Fiedler, S., Stahr, K., 2005. Indirect nitrous oxide emission from a nitrogen saturated spruce forest and general accuracy of the IPCC methodology. Atmos. Environ. 39, 5959–5970.
Huebsch, M., Horan, B., Blum, P., Richards, K.G., Grant, J., Fenton, O., 2013. Impact of local weather conditions and agronomic practices on groundwater nitrogen content in a karst aquifer on an intensive dairy farm in Southern Ireland. Agric. Ecosyst. Environ. 179, 187–199.
Intergovernmental Panel on Climate Change (IPCC), 2006. N_2O emissions from managed soils, and CO_2 emissions from lime and urea application. In: Eggleston, H.S., Buendia, I., Miwa, K., Ngara, T., Takabe, K. (Eds.), Chapter II: Agriculture, Forestry and Other Land use2006 IPCC Guidelines for National Greenhouse Gas Inventories vol. 4. IGES, Hayama, Japan.
International Panel on Climate Change (IPCC), 1997. Revised 1996 IPCC Guidelines for National Greenhouse gas Inventories, Reference Manual vol. 3. Organisation for Economic Cooperation and Development, Paris.
Jahangir, M.M.R., Johnston, P., Khalil, M., Richards, K.G., 2012a. Linking hydrogeochemistry to nitrate abundance in groundwater in agricultural settings in Ireland. J. Hydrol. 448, 212–222.
Jahangir, M.M.R., Johnston, P., Khalil, M., Grant, J., Somers, C., Richards, K.G., 2012b. Evaluation of headspace equilibration methods for quantifying greenhouse gases in groundwater. J. Environ. Manag. 111, 208–212.
Jahangir, M.M.R., Johnston, P., Barrett, M., Khalil, M., Groffman, P., Boeckx, P., Fenton, O., Murphy, J., Richards, K.G., 2013. Denitrification and indirect N_2O emissions in groundwater: hydrologic and biogeochemical influences. J. Contam. Hydrol. 152, 70–81.
Jahangir, M.M.R., Minet, E.P., Johnston, P., Premrov, A., Coxon, C.E., Hackett, R., Richards, K.G., 2014. Mustard catch crop enhances denitrification in shallow groundwater beneath a spring barley field. Chemosphere 103, 234–239.
Jahangir, M.M.R., Richards, K.G., Healy, M.G., Gill, L., Müller, C., Johnston, P., Fenton, O., 2016. Carbon and nitrogen dynamics and greenhouse gas emissions in constructed wetlands treating wastewater: a review. Hydrol. Earth Syst. Sci. 20, 1–15.
Kana, T.M., Darkangelo, C., Hunt, M.D., Oldham, J.B., Bennett, G.E., Cornwell, J.C., 1994. Membrane inlet mass spectrometer for rapid high-precision determination of N_2, O_2, and Ar in environmental water samples. Anal. Chem. 66, 4166–4170.
Kendall, C., Elliott, E.M., Wankel, S.D., 2007. Tracing Anthropogenic Inputs of Nitrogen to Ecosystems. Stable Isotopes in Ecology and Environmental Science 2 pp. 375–449.
Korom, S.F., 1992. Natural denitrification in the saturated zone: a review. Water Resour. Res. 28, 1657–1668.
Li, D., Lanigan, G., Humphreys, J., 2011. Measured and simulated nitrous oxide emissions from ryegrass-and ryegrass/white clover-based grasslands in a moist temperate climate. PLoS One 6, e26176.
Li, D., Watson, C.J., Yan, M.J., Lalor, S., Rafique, R., Hyde, B., Lanigan, G., Richards, K.G., Holden, N.M., Humphreys, J., 2013. A review of nitrous oxide mitigation by farm nitrogen management in temperate grassland-based agriculture. J. Environ. Manag. 128, 893–903.
Liao, L., Green, C.T., Bekins, B.A., Böhlke, J., 2012. Factors controlling nitrate fluxes in groundwater in agricultural areas. Water Resour. Res. 48 (6).
Mellander, P.E., Melland, A.R., Jordan, P., Wall, D.P., Murphy, P.N., Shortle, G., 2012. Quantifying nutrient transfer pathways in agricultural catchments using high temporal resolution data. Environ. Sci. Pol. 24, 44–57.
Mellander, P.-E., Melland, A., Murphy, P., Wall, D., Shortle, G., Jordan, P., 2014. Coupling of surface water and groundwater nitrate-N dynamics in two permeable agricultural catchments. J. Agric. Sci. 152, 107–124.
Mengis, M., Schif, S., Harris, M., English, M., Aravena, R., Elgood, R., Maclean, A., 1999. Multiple geochemical and isotopic approaches for assessing ground water NO_3^- elimination in a riparian zone. Groundwater 37, 448–457.
Mosier, A., Kroeze, C., Nevison, C., Oenema, O., Seitzinger, S., Van Cleemput, O., 1999. An overview of the revised 1996 IPCC guidelines for national greenhouse gas inventory methodology for nitrous oxide from agriculture. Environ. Sci. Pol. 2, 325–333.
Mühlherr, I.H., Hiscock, K.M., 1998. Nitrous oxide production and consumption in British limestone aquifers. J. Hydrol. 211, 126–139.
Pabich, W.J., Valiela, I., Hemond, H.F., 2001. Relationship between DOC concentration and vadose zone thickness and depth below water table in groundwater of Cape Cod, USA. Biogeochemistry 55, 247–268.
Panno, S.V., Hackley, K.C., Kelly, W.R., Hwang, H.-H., 2006. Isotopic evidence of nitrate sources and denitrification in the Mississippi River, Illinois. J. Environ. Qual. 35, 495–504.
Penman, J., 2000. Good Practice Guidance and Uncertainty Management in National Greenhouse gas Inventories.
Premrov, A., Coxon, C.E., Hackett, R., Kirwan, L., Richards, K.G., 2012. Effects of over-winter green cover on groundwater nitrate and dissolved organic carbon concentrations beneath tillage land. Sci. Total Environ. 438, 144–153.
Reay, D.S., Smith, K.A., Edwards, A.C., Hiscock, K.M., Dong, L.F., Nedwell, D.B., 2005. Indirect nitrous oxide emissions: revised emission factors. Environ. Sci. 2, 153–158.
Richards, K.G., Jahangir, M.M.R., Drennan, M., Lenehan, J.J., Connolly, J., Brophy, C., Carton, O.T., 2015. Effect of an agri-environmental measure on nitrate leaching from a beef farming system in Ireland. Agric. Ecosyst. Environ. 202, 17–24.
Rissmann, C., 2011. Regional mapping of groundwater denitrification potential and aquifer sensitivity. Technical Report for Environment Southland.
Rivett, M.O., Buss, S.R., Morgan, P., Smith, J.W., Bemment, C.D., 2008. Nitrate attenuation in groundwater: a review of biogeochemical controlling processes. Water Res. 42, 4215–4232.
Sawamoto, T., Nakajima, Y., Kasuya, M., Tsuruta, H., Yagi, K., 2005. Evaluation of emission factors for indirect N_2O emission due to nitrogen leaching in agro-ecosystems. Geophys. Res. Lett. 32.
Schipper, L.A., Vojvodić-Vuković, M., 2001. Five years of nitrate removal, denitrification and carbon dynamics in a denitrification wall. Water Res. 35 (14), 3473–3477.
Seitzinger, S., Harrison, J.A., Böhlke, J., Bouwman, A., Lowrance, R., Peterson, B., Tobias, C., Drecht, G.V., 2006. Denitrification across landscapes and waterscapes: a synthesis. Ecol. Appl. 16, 2064–2090.
Sigman, D., Casciotti, K., Andreani, M., Barford, C., Galanter, M., Böhlke, J., 2001. A bacterial method for the nitrogen isotopic analysis of nitrate in seawater and freshwater. Anal. Chem. 73, 4145–4153.
Soussana, J., Allard, V., Pilegaard, K., Ambus, P., Amman, C., Campbell, C., Ceschia, E., Clifton-Brown, J., Czóbel, S., Domingues, R., 2007. Full accounting of the greenhouse gas (CO_2, N_2O, CH4) budget of nine European grassland sites. Agric. Ecosyst. Environ. 121, 121–134.
Spalding, R.F., Exner, M.E., 1993. Occurrence of nitrate in groundwater—a review. J. Environ. Qual. 22, 392–402.
Starr, R.C., Gillham, R.W., 1993. Denitrification and organic carbon availability in two aquifers. Groundwater 31, 934–947.
Tesoriero, A.J., Puckett, L.J., 2011. O_2 reduction and denitrification rates in shallow aquifers. Water Resour. Res. 47.
Thayalakumaran, T., Bristow, K.L., Charlesworth, P.B., Fass, T., 2008. Geochemical conditions in groundwater systems: implications for the attenuation of agricultural nitrate. Agric. Water Manag. 95, 103–115.
Thayalakumaran, T., Lenahan, M.J., Bristow, K.L., 2015. Dissolved organic carbon in groundwater overlain by irrigated sugarcane. Groundwater 53, 525–530.
Tsushima, K., Ueda, S., Ogura, N., 2002. Nitrate loss for denitrification during high frequency research in floodplain groundwater of the Tama River. Water Air Soil Pollut. 137, 167–178.
Vidon, P., Hill, A.R., 2005. Denitrification and patterns of electron donors and acceptors in eight riparian zones with contrasting hydrogeology. Biogeochemistry 71, 259–283.
Vilain, G., Garnier, J., Tallec, G., Tournebize, J., 2012. Indirect N_2O emissions from shallow groundwater in an agricultural catchment (Seine Basin, France). Biogeochemistry 111, 253–271.
Vitousek, P.M., Aber, J.D., Howarth, R.W., Likens, G.E., Matson, P.A., Schindler, D.W., Schlesinger, W.H., Tilman, D.G., 1997. Human alteration of the global nitrogen cycle: sources and consequences. Ecol. Appl. 7, 737–750.
Von Der Heide, C., Böttcher, J., Deurer, M., Duijnisveld, W.H., Weymann, D., Well, R., 2009. Estimation of indirect nitrous oxide emissions from a shallow aquifer in northern Germany. J. Environ. Qual. 38, 2161–2171.
Wassenaar, L.I., 1995. Evaluation of the origin and fate of nitrate in the Abbotsford Aquifer using the isotopes of ^{15}N and ^{18}O in NO_3^-. Appl. Geochem. 10, 391–405.
Well, R., Eschenbach, W., Flessa, H., Von Der Heide, C., Weymann, D., 2012. Are dual isotope and isotopomer ratios of N_2O useful indicators for N_2O turnover during denitrification in nitrate-contaminated aquifers? Geochim. Cosmochim. Acta 90, 265–282.
Weymann, D., Well, R., Flessa, H., Heide, C., Deurer, M., Meyer, K., Konrad, C., Walther, W., 2008. Groundwater N_2O emission factors of nitrate-contaminated aquifers as derived from denitrification progress and N_2O accumulation. Biogeosciences 5, 1215–1226.
Yanai, J., Sawamoto, T., Oe, T., Kusa, K., Yamakawa, K., Sakamoto, K., Naganawa, T., Inubushi, K., Hatano, R., Kosaki, T., 2003. Spatial variability of nitrous oxide emissions and their soil-related determining factors in an agricultural field. J. Environ. Qual. 32, 1965–1977.
Young, C., Kroeger, K.D., Hanson, G., 2013. Limited denitrification in glacial deposit aquifers having thick unsaturated zones (Long Island, USA). Hydrogeol. J. 21, 1773–1786.